HHS Public Access

Author manuscript

Nat Immunol. Author manuscript; available in PMC 2015 April 29.

Published in final edited form as:

Nat Immunol. 2015 January ; 16(1): 118–128. doi:10.1038/ni.3036.

TLR7 induces anergy in human CD4+ T cells

Margarita Dominguez-Villar[1,*], **Anne-Sophie Gautron**[1], **Marine de Marcken**[1], **Marla J. Keller**[2], and **David A. Hafler**[1,*]

[1]Departments of Neurology and Immunobiology, Yale School of Medicine, New Haven, Connecticut 06520

[2]Albert Einstein College of Medicine and Montefiore Medical Center, Bronx, NY 10461

Abstract

Pattern recognition of microbes by Toll-like receptors (TLR) is critical for innate immune system activation. Although TLRs are expressed in human $CD4^+$ T cells, their function is not well understood. Here we demonstrate that engaging TLR7 in $CD4^+$ T cells induces intracellular calcium flux with activation of an NFATc2-dependent anergic gene expression program and T cell non-responsiveness. As chronic infections with RNA viruses such as HIV-1 induce profound $CD4^+$ T cell dysfunction, we examined the role of TLR7-induced anergy in HIV-1 infection. *TLR7* gene silencing markedly decreases the frequency of HIV-1-infected $CD4^+$ T cells and restores cell responsiveness in those $HIV\text{-}1^+$ $CD4^+$ T cells. These results elucidate a previously unknown function for microbial pattern recognition receptors to down-regulate immune responses.

Toll-like receptors (TLRs) represent the major pathway by which microorganisms interact with host cells. They are a family of highly conserved pattern recognition receptors that recognize distinct pathogen-associated molecular patterns (PAMPs) that are conserved in specific classes of microorganisms[1]. The human TLR family consists of at least 10 members that can be classified into two different groups based on their cellular location. Intracellular TLR (TLR3, 7, 8 and 9) recognize nucleic acids; TLR7 and TLR8 recognize single-stranded RNA[2, 3], whereas TLR3 and TLR9 are receptors for double-stranded RNA and DNA, respectively. In contrast, cell surface TLRs (TLR1, 2, 4, 5 and 6) recognize different components of bacteria[1]. In mice, although TLR7 and TLR8 are expressed at low levels in $CD4^+$ T cells, there are species-specific differences in the recognition of ligands[3] as well as in their functionality. Specifically, murine TLR7 and human TLR8 mediate species-specific recognition of GU-rich ssRNA. It has been suggested that in contrast to human, mice TLR8 is not functional, TLR7 being the only TLR that recognizes single-stranded RNA[4]. The expression and signaling pathways triggered by stimulating the TLR have been primarily described in antigen presenting cells (APC) that leads to activation of APC with inflammatory and antiviral cytokine secretion[1, 5]. Although predominantly studied in APC,

*Correspondence to: margarita.dominguez-villar@yale.edu and david.hafler@yale.edu.

Author contribution

MDV designed and performed the experiments, analyzed data and wrote the manuscript. ASG and MdM performed experiments, MK provided HIV-1 samples and DAH assisted with design of experiments, supervised the project and wrote the manuscript.

The authors declare no competing financial interests.

several reports have described the expression of TLR on lymphocytes[6], and specifically on $CD4^+$ T cells. As with APC, these studies indicate that TLR engagement acts as a positive costimulatory signal that increases the secretion of pro-inflammatory cytokines, proliferation and cell survival[7, 8].

While TLRs are central in the early host immune response to acute viral infection, more chronic infectious diseases are characterized by the inability of the host immune system to mount a strong, long-lasting response against the infectious agent. In particular, it has been shown with RNA viral infections such as with Hepatitis C (HCV) and Human Immunodeficiency Virus (HIV-1) that $CD4^+$ T helper cell- and $CD8^+$ cytotoxic T-cell-mediated immune responses determine the outcome of the infection, with chronic infections correlating with late, transient, or narrowly focused $CD4^+$ and $CD8^+$ T cell responses[9, 10, 11]. Several studies have demonstrated that there is impairment with activation and/or function of T cells in HIV-1 infection. Specifically, $CD4^+$ T cells from chronically HIV-1-infected patients display an anergic phenotype with defects in proliferation and IL-2 and interferon-γ (IFN--γ) secretion {Prince, 1988 #383;Gruters, 1990 #385}. The mechanisms by which RNA viruses impair T cell function are not well understood.

Here, we describe a previously unrecognized pathway of TLR-mediated negative regulation of both $CD4^+$ T cell activation and cytokine production. Engaging TLR7 expressed in $CD4^+$ T cells results in complete anergy by inducing an intracellular calcium flux with activation of an NFATc2-dependent anergic gene expression program with subsequent T cell non-responsiveness that is reversed with shRNA knockdown of *TLR7*. To examine potential physiologic relevance, shRNA knockdown of the *TLR7* gene decreased the frequency of *in vitro* HIV-1-infected $CD4^+$ T cells and restored T cell responsiveness in those *in vitro* $HIV\text{-}1^+$ $CD4^+$ T cells. These results elucidate a previously unknown function for microbial pattern recognition receptors to down-regulate immune responses, inducing anergy by interfering with secondary costimulation signals in the presence of T cell receptor signaling.

Results

TLR7 ligation inhibits $CD4^+$ T cell activation upon TCR stimulation

While examining the potential costimulatory role of TLR on $CD4^+$ T cells, we observed that entry of $CD4^+$ T cells into cell cycle with T cell receptor (TCR) cross-linking and anti-CD28 was blocked by TLR7 co-engagement (Fig. 1a–b and Supplementary Fig. 1a–b). The synthetic TLR7 agonist Imiquimod (IMQ) dramatically reduced the proliferation of $CD4^+$ T cells as well as the secretion of IFN-γ and IL-17 as compared to control cells in a dose-dependent fashion (Fig. 1c–e and Supplementary Fig. 1c–d). This inhibitory effect was observed as soon as 12 hours after activation, with a significant decrease in the induction of *IL2*, *IFNG* and *IL4* gene expression with IMQ treatment (Supplementary Fig. 1e). Concentrations up to 15 μg/ml IMQ were examined with no effect on cell viability (data not shown). The decrease in proliferation correlated with a decrease in the secretion of the cytokines IFN-γ, IL-17, IL-2 and IL-4 as measured by ELISA at day 3 after stimulation (Fig. 1c). This reduction of cytokine secretion was confirmed at the single cell level, as the frequency of cytokine-producing cells was also diminished in a dose-dependent manner with increasing doses of IMQ in the cultures (Fig. 1d–e). Furthermore, $CD4^+$ T cell stimulation in

the presence of IMQ inhibited the expression of activation markers such as CD25, CD69 and CD137, measured 48 hours after activation (Fig. 1f). Of note, the effect of IMQ was not related to the conversion of $CD4^+$ T cells into a regulatory T (T_{reg}) cell population, as neither FOXP3 protein expression nor IL-10 secretion was increased in the presence of IMQ (data not shown). The unresponsive phenotype observed was not due to an indirect effect of TLR7 on T_{reg} cells, as we obtained the same results with sorted T_{reg}-depleted $CD4^+$ T cells (sorted $CD4^+CD25^{+/lo}CD127^+$, data not shown). Only TLR9 stimulation with the synthetic ligand ODN2006 also decreased the frequency of proliferating $CD4^+$ T cells, but to a lesser extent than TLR7 (Supplementary Fig. 1a). The effect observed was not due to an indirect effect of TLR7 triggering on contaminant APC in the culture, as IMQ exerted the same effect on T cell clones grown from a healthy donor (Supplementary Fig. 2).

To confirm the specificity of our results, $CD4^+$ T cells were stimulated in the presence of other synthetic TLR7 ligands, such as Loxoribine (Loxo), CL264, or Gardiquimod (GDQ, Fig. 2). The three ligands tested induced a significant decrease in $CD4^+$ T cell proliferation as compared to a vehicle control (Fig. 2a–b), with GDQ and Loxoribine inhibiting proliferation to a degree comparable to IMQ treatment. IL-2, IFN-γ, IL-4 and IL-17 secretion was also inhibited after stimulation in the presence of each of the three ligands, as measured by ELISA after 3 days in culture (Fig. 2c). The specificity of the phenotype observed was further demonstrated by TLR7 silencing on $CD4^+$ T cells (Fig. 2d). While non-target-transduced control $CD4^+$ T cells responded to IMQ treatment by decreasing the secretion of IFN-γ and IL-2, TLR7-silenced $CD4^+$ T cells produced similar concentrations of IFN-γ and IL-2 as compared to vehicle upon IMQ stimulation (Fig. 2e). Both TLR7 and TLR8 are expressed in human $CD4^+$ T cell subpopulations[6, 8], but although reports suggest that both TLR7 and TLR8 recognize single-stranded RNA as their natural ligand in APC[2, 3], no such effect was observed when the TLR8 ligand (ssRNA40 transfected in LyoVec™) was used in these experiments in parallel with TLR7 ligands (Fig. 2f–g). Instead, T cell stimulation in the presence of ssRNA40 significantly increased the production of IFN-γ and inhibited the secretion of IL-4 by $CD4^+$ T cells (Fig. 2g), showing no effect on proliferation (Fig. 2f). Vehicle (LyoVec™) did not have any effect on cytokine secretion or proliferation under the experimental conditions examined (data not shown). The same results were obtained with CL075, another predominantly TLR8 ligand (data not shown). These data are in agreement with a previous report[8] and suggest that despite sharing ligands, the signaling pathways that TLR7 and TLR8 trigger on $CD4^+$ T cells lead to different phenotypic outcomes.

TLR7 ligation induces the activation and maturation of APC, with upregulation of activation markers and secretion of proinflammatory cytokines[12, 13, 14]. In agreement with published data, $CD14^+$ monocytes isolated from the same donors stimulated in the presence or absence of IMQ showed an activated phenotype, with upregulation of HLA-DR, CD80 and CD25, and downregulation of CD86 protein expression (Supplementary Fig. 3a). Upon IMQ stimulation, $CD14^+$ monocytes also secreted the pro-inflammatory cytokines IL-6, TNF and IL-1β and decreased IL-10 secretion (Supplementary Fig. 3b), whereas there was no effect observed on monocyte proliferation (data not shown), suggesting that IMQ stimulation on $CD4^+$ T cells and $CD14^+$ monocytes leads to completely different outcomes.

To confirm the specificity of the unresponsive phenotype driven by TLR7 signaling, $CD4^+$ T cells were stimulated in the presence of an shRNA specific for TLR7 or a non-target shRNA as control. After 5 days of culture, we confirmed that protein and RNA silencing efficiency was >80% (Fig. 2d). Resting TLR7-silenced $CD4^+$ T cells were stimulated with anti-CD3 and anti-CD28 in the presence or absence of IMQ and IL-2 and IFN-γ secretion was measured. While $CD4^+$ T cells transduced with a non-target shRNA showed a decrease in the production of IL-2 and IFN-γ secretion with IMQ, this effect was abolished when the cells expressed a shRNA specific for TLR7, confirming that the unresponsive state observed in T cells in the presence of IMQ is TLR7-specific (Fig. 2e).

TLR7 stimulation induces calcium-NFATc2-driven $CD4^+$ T cell anergy

The inhibition of proliferation, cytokine secretion and activation of $CD4^+$ T cells upon stimulation in the presence of TLR7 ligands resembled the unresponsive phenotype that characterizes clonal anergy[15]. Different model systems have been used to induce clonal anergy, including treatment with the calcium ionophore ionomycin[16, 17] and the activation of calcium signaling in the absence of activating signals in costimulatory signaling pathways is common in all these models. Thus, the main characteristic of an anergizing stimulus is its ability to induce an unopposed increase in intracellular calcium concentrations[17]. To test the hypothesis that TLR7 signaling on $CD4^+$ T cells was inducing clonal anergy, sorted $CD4^+$ T cells were stained with the ratiometric calcium indicator Indo-1AM and treated with different doses of IMQ (Fig. 3a). IMQ induced a significant and sustained (maintained for at least 20 minutes) increase in intracellular calcium concentration in a dose-dependent manner that was TLR7-specific, as blocking TLR7 with the specific inhibitory sequence IRS661[18] impaired the increase in calcium concentration upon IMQ stimulation (Fig. 3b and Supplementary Fig. 4a). The increase in intracellular calcium concentration was not observed when the cells were stimulated with the TLR8 agonist ssRNA40 or other ligands for intracellular TLRs; Poly(I:C) for TLR3 and ODN2006 for TLR9 (Fig. 3a, Supplementary Fig. 4b). As a positive control, cells were treated with the calcium ionophore ionomycin, which has been used as an anergy-inducing agent in *in vitro* experiments[17, 19] (Fig. 3a and Supplementary Fig. 4a).

An immediate consequence of increased concentration of intracellular calcium is the activation of the nuclear factor of activated T-cells (NFATc2), a transcription factor that is highly phosphorylated in resting cells and becomes dephosphorylated by the calcium/calmodulin-dependent phosphatase calcineurin when the concentration of intracellular calcium is increased[20, 21]. To examine whether IMQ stimulation induced the dephosphorylation of NFATc2, we stimulated $CD4^+$ T cells with IMQ and purified total protein extracts at 0, 45 and 90 minutes (Fig. 3c). Immunoblot analysis with an anti-NFATc2 antibody showed that IMQ dephosphorylated NFATc2, and these results were confirmed using a phospho-specific anti-NFATc2 antibody with total extracts from $CD4^+$ T cells stimulated with IMQ for 40 minutes (Fig. 3c). Nuclear and cytoplasmic protein extracts were also used to further confirm NFATc2 translocation upon IMQ stimulation (data not shown).

NFATc2 translocates to the nucleus with dephosphorylation where it becomes transcriptionally active[22]. This NFATc2 translocation to the nucleus in the absence of a concomitant costimulation signal leads to the transcription of a set of NFATc2-dependent, anergy-related genes that are different from those upregulated with full activation in the presence of a costimulatory signal[17]. To examine whether TLR7 stimulation and subsequent NFATc2 dephosphorylation induces the expression of anergy-related genes, $CD4^+$ T cells were incubated for 2–16 hours with IMQ in the presence or absence of the TLR7 inhibitory sequence IRS661 and RNA was isolated to examine the hypothesis that TLR7 engagement induced the expression of anergy-related genes previously described[17]. As a control for anergy-related gene expression, $CD4^+$ T cells were incubated with either ionomycin plus PMA (a non-anergic stimulus) or ionomycin alone (an anergic stimulus)[17] (Supplementary Fig. 5). Ten of the 12 anergy-related genes examined were significantly upregulated in IMQ-stimulated cells as compared to the control PMA plus ionomycin stimulation (Fig. 3d and Supplementary Fig. 5). The effect observed in the regulation of these genes was TLR7-specific, as preincubation of $CD4^+$ T cells with IRS661 before IMQ treatment abrogated the increase in anergy-related gene expression. Furthermore, the expression of other genes that have been functionally related to the establishment and maintenance of the anergic phenotype and are NFAT targets, such as *SIRT1*[23], *ITCH*[24], *CBLB*[24, 25], *DGKA*[26], *EGR2* and *EGR3*[27] was also examined, and all of them but *EGR2* showed a significant upregulation upon IMQ treatment (Fig. 3d). Our data suggest that IMQ induces clonal anergy in $CD4^+$ T cells by the increase in intracellular calcium concentration and activation of an NFATc2-dependent anergic gene expression program. To further examine the role of NFATc2 on TLR7-induced T cell anergy, two shRNA were used to silence NFATc2 (Fig. 3e and Supplementary Fig. 6), and IMQ was used to induce anergy on resting $CD4^+$ T cells after NFATc2 knockdown. After 3 days in culture, cells transduced with a non-target shRNA and stimulated with IMQ significantly reduced the production of IL-2 and IFN-γ while cells transduced with NFATc2 shRNA were not affected by IMQ treatment, suggesting that NFATc2 is necessary for the anergic phenotype driven by TLR7 signaling in $CD4^+$ T cells. IMQ treatment did not have an effect on NFATc2 gene expression (Supplementary Fig. 6a). In agreement with these data and previous observations[17], IMQ treatment failed to upregulate the expression of anergy-related genes (*KMD6B, IKZF1, GRG4, RAB10*) in NFATc2-knockdown $CD4^+$ T cells as compared to non-target transduced cells, confirming that this gene expression program driven by IMQ treatment on $CD4^+$ T cells is largely NFATc2-dependent (Supplementary Fig. 6b).

As previously published in the ionomycin-induced anergy model[17], we hypothesized that pretreatment of $CD4^+$ T cells with IMQ would be sufficient to diminish their subsequent cytokine secretion and proliferative response to stimulation with both T cell receptor crosslinking and a co-stimulatory signal through CD28. Memory $CD4^+$ T cells were pre-treated with IMQ for two hours and rested for 12 hours after washout to remove traces of IMQ and then stimulated with anti-CD3 and anti-CD28 for 3 days. IMQ-pretreated cells showed a significantly decreased production of both IL-2 and IFN-γ that was not observed on IRS661 pretreated cells (Fig. 3f). No significant changes in cell viability were observed upon IMQ pretreatment. Again, the pro-anergic effect of IMQ could be prevented by pretreatment with the TLR7 antagonist IRS661. These data suggest that IMQ induces clonal

anergy on CD4$^+$ T cells by inducing calcium-dependent activation of NFATc2 and subsequent expression of anergy-related genes.

TLR7 signaling interferes with AP-1 costimulatory signals

TLR7 signaling has predominantly been studied in APCs where it is linked to IRF7, NF-κB and JNK activation through either MyD88-IRAK4-dependent or –independent pathways[1]. In order to examine the consequences of TLR7 signaling on CD4$^+$ T cells in relation to 'conventional' TLR signaling, *ex vivo* isolated CD4$^+$ T cells from healthy individuals were stimulated with IMQ and the phosphorylation status of IRAK4, JNK, NFkB (p65) and p38 MAPK was examined by flow cytometry (Fig. 4). In agreement with previous reports on other cell types, TLR7 stimulation with IMQ induced the phosphorylation of IRAK4, NFκB and p38 at different time points as compared to vehicle. Preincubation with IRS661 prior to IMQ stimulation inhibited the phosphorylation of these molecules, suggesting that the effect observed was TLR7-specific. IRS661 incubation by itself did not have any effect on protein phosphorylation (data not shown). TLR7 engagement decreased the basal levels of phosphorylated JNK. One of the targets that are phosphorylated by activated JNK is Jun, a component of AP-1, which is an essential transcription factor involved in costimulatory signal transduction[17]. We hypothesized that inhibition of JNK activity by IMQ could explain, at least in part, the anergic phenotype observed in CD4$^+$ T cells after IMQ stimulation in the presence of full stimulation with TCR and costimulatory signals (Fig. 1 and Fig. 2). To test this hypothesis, CD4$^+$ T cells were stimulated with PMA plus ionomycin in the presence or absence of IMQ, and we examined the phosphorylation status of JNK and Jun at different time points. NF-κB and p38 were used as positive controls. Although IMQ treatment did not show an additive effect on NF-κB phosphorylation with stimulation, IMQ further increased p38 phosphorylation (Fig. 5a). Of note, upon PMA plus ionomycin stimulation, JNK phosphorylation was inhibited by IMQ and this decrease in JNK activity was accompanied by a decrease in Jun phosphorylation. Moreover, IMQ both decreased JNK and Jun activity measured by phosphorylation after activation, and decreased *JUN* gene expression (Fig. 5b). These data support the hypothesis that IMQ treatment both induces anergy on CD4$^+$ T cells and interferes with costimulatory signals during T cell stimulation. The decrease in CD69 and CD137 expression (both AP-1 transcriptional targets[28, 29], Fig. 1f) observed after stimulation in the presence of IMQ further supports this hypothesis.

TLR7-Ca^{2+} signaling blockade inhibits *in vitro* HIV-1 infection

To examine the potential biologic and clinical relevance of these observations in *ex vivo* and *in vitro* model systems, we determined whether TLR7 engagement by a single-stranded RNA virus[2, 3] could mediate CD4$^+$ T cell anergy. CD4$^+$ T cell responses from chronically HIV-1-infected patients are impaired and insufficient to clear the virus while displaying features of anergy[30, 31, 32, 33]. Several viral proteins have been shown to induce a state of T cell non-responsiveness {Subramanyam, 1993 #375;Faith, 1992 #376} that precedes CD4$^+$ T cell loss[30] in HIV-1 patients. We hypothesized that virus-CD4$^+$ T cell interaction through TLR7 would be responsible, at least in part, for the anergic phenotype observed in HIV-1-infected CD4$^+$ T cells from patients. First, we isolated CD4$^+$ T cells from four healthy individuals and examined their ability to produce IL-2 and IFN-γ seven days after *in vitro* infection with physiological concentrations of the replication-competent DsRed-tagged

HIV-1_{NL-D}, derived from the prototype HIV-1_{NL432} virus (MOI 0.001)[34, 35]. In agreement with published reports, HIV-1 infection markedly decreased the ability of viable $CD4^+$ T cells to produce IL-2 and IFN-γ after stimulation (Supplementary Fig. 7). This decrease in cytokine secretion was not observed only in the bulk T cell population infected with the virus, but specifically in HIV-1-infected cells, suggesting that the direct interaction of the virus with the infected $CD4^+$ T cell rendered $CD4^+$ T cells unresponsive.

To test the hypothesis that TLR7 signaling in $CD4^+$ T cells is accounting in part for the anergic phenotype after HIV-1 infection, we used two shRNA specific for TLR7 (clones 3 and 4) or a non-target shRNA as control, to silence TLR7 on *ex vivo* isolated $CD4^+$ T cells from healthy donors (Fig. 6). After two days, TLR7-deficient $CD4^+$ T cells were infected with concentrations of HIV-1 within the physiological range[34] (MOI 0.001) and the frequency of infected cells as well as their ability to produce proinflammatory cytokines was measured every 48 hours for a total of 11 days. Although non-target transduced $CD4^+$ T cells were infected with HIV-1 to a similar extent as compared to non-transduced cells, TLR7-deficient cells showed a marked decrease in the frequency of HIV-1-infected $CD4^+$ T cells at all time points examined (Fig. 6a–b). This decrease in the frequency of HIV-1^+ cells was not due to a specific increase in cell death on TLR7-silenced cells, as there were no differences in the frequency of early and late apoptotic $CD4^+$ T cells after infection as compared to the control (non-target-transduced $CD4^+$ T cells, Supplementary Fig. 8). The role of TLR7 in decreasing the HIV-1 infection rate was further confirmed by TLR7 blockade on $CD4^+$ T cells from healthy donors with different doses of IRS661 prior *in vitro* infection (Fig. 6c–d). Moreover, cytokine secretion of HIV-1-infected cells was significantly different in non-target transduced cells as compared to TLR7-deficient cells. Although HIV-1-infected cells in non-target-transduced $CD4^+$ T cell culture displayed decreased amounts of IL-2 and IFN-γ protein, the low frequency of $CD4^+$ T cells infected with HIV-1 in TLR7-deficient cells secreted significantly more IL-2 and IFN-γ than non-target-transduced cells, suggesting that the anergic phenotype is not observed in TLR7-deficient cells after infection (Fig. 6e–f). To confirm this observation we examined the expression of anergy-related genes in *in vitro* HIV-1-infected $CD4^+$ T cells from five healthy donors in the presence of IRS661 (to inhibit TLR7) or a control sequence at day seven after infection (Fig. 6g). Sorted HIV-1^+CD4^+ T cells showed an increased expression of 8 out of the 12 anergy-related genes examined, while HIV-1^+CD4^+ T cells sorted from IRS661-treated cultures did not upregulate any of these genes at the time point analyzed. The expressions of other genes that have been functionally implicated in anergy such as *ITCH*, *DGKA*, *CBLB* and *SIRT1* were also upregulated in HIV-1^+CD4^+ T cells, but not in IRS661-treated HIV-1^+ T cells (data not shown). These data suggest that HIV-1 interaction with TLR7 is responsible, at least in part, for the anergic phenotype observed in infected HIV-1^+CD4^+ T cells.

We examined the role of intracellular calcium and NFATc2-activated gene expression signaling events we observed by TLR7 engagement with IMQ, after *in vitro* HIV-1 infection. We hypothesized that intracellular calcium blockade and NFATc2 silencing would lead to a decrease in the frequency of HIV-1^+ T cells even in the presence of a functional TLR7. To induce a calcium blockade, we pre-incubated $CD4^+$ T cells with the chelation agent Quin-2 AM[36] before HIV-1 infection (Fig. 6h). Calcium chelation significantly

decreased the frequency of viable cells even at the lowest chelating agent concentration, perhaps due to the essential role of calcium in many cellular processes. Nevertheless, the remaining viable $CD4^+$ T cells in culture showed a marked decrease in the frequency of HIV-1^+ T cells, in agreement with previous investigations indicating a role for calcium in the HIV-1 life cycle[37]. NFATc2 was then silenced with either two different shRNA or blocked with VIVIT peptide, which interferes with calcineurin-NFATc2 interaction, inhibiting NFAT dephosphorylation[38]. In both cases, the absence of functional NFATc2 led to a significant decrease in the frequency of HIV-1-infected T cells (Fig. 6i–j), indicating a role for NFATc2 in HIV-1 infection, as previously suggested[39]. These data suggest that calcium-dependent NFATc2 activation upon TLR7 triggering is involved in HIV-1 infection *in vitro*.

Calcium-induced anergy favors HIV-1 replication

Based on the decreased infection rate on TLR7-silenced cells and the non-anergic phenotype of the infected $CD4^+$ TLR7-deficient T cells, we hypothesized that the anergic state induced by TLR7 stimulation during HIV-1 infection would be a necessary step for HIV-1 to replicate in the host. In the absence of TLR7 signaling, the virus would not be able to render the infecting cell anergic and long-term infection would not occur. To examine this hypothesis, we induced anergy via the TLR7 pathway on $CD4^+$ T cells from healthy donors with different doses of IMQ and subsequently infected them with HIV-1 for 7 days (Fig. 7a–b). Of note, the frequency of HIV-1-infected $CD4^+$ T cells directly correlated with the concentration of IMQ used, the increase in intracellular calcium and thus with the degree of anergy in the culture, suggesting that calcium-induced anergy favors HIV-1 infection. Moreover, anergy induction through other well established *in vitro* methods, such as ionomycin treatment (Fig. 7c–d) or anti-CD3 stimulation without costimulatory signals (Fig. 7e–f) prior to HIV-1 infection also increased the frequency of HIV-1^+ infected cells. These data support the hypothesis that HIV-1-induced anergy by TLR7 ligation and increase in intracellular calcium concentration is a prerequisite for productive HIV-1 infection. To further examine whether inhibiting TLR7-induced anergy would affect the frequency of HIV-1-infected cells, we added either the calcineurin inhibitor cyclosporine A or concentrations of IL-2 that have been shown to reverse anergy in several *in vitro* settings[17] prior to *in vitro* HIV-1 infection. Although the addition of IL-2 six hours before HIV-1 infection did not affect the frequency of HIV-1-infected cells, perhaps due to response kinetics, the broad spectrum of IL-2 functions or the inability of IL-2 to rescue $CD4^+$ T cells from TLR7-induced anergy (data not shown), blocking anergy with cyclosporine A significantly decreased the frequency of HIV-1^+ T cells (Fig. 7g), further supporting the hypothesis that HIV-1-induced anergy is necessary for productive HIV-1 infection.

TLR7 inhibition reduces HIV-1 in patient T cells *ex vivo*

We then wished to directly examine the role of TLR7 in $CD4^+$ T cells from HIV-1-infected patients. Specifically, based on the *in vitro* model system with DsRed-tagged HIV-$1_{NL\text{-}D}$, we hypothesized that inhibition of the TLR7 pathway in $CD4^+$ T cells from HIV-1-infected patients would decrease the infection rate. $CD4^+$ T cells isolated from nine HIV-1 infected patients (Supplementary Table 1) were stimulated in the presence of IRS661 (Fig. 8a–b) or were transduced with two TLR7-specific shRNA (Fig. 8c–d) with supernatant collections

every three days for a total of 14 days to measure virus concentration by p24 ELISA. TLR7 inhibition by IRS661 strongly decreased the concentration of the HIV-1 signature protein p24 in culture and similar results were obtained when the cells were transduced with two TLR7-specific shRNA. Healthy donor $CD4^+$ T cells were assayed in parallel as a negative control, with no detectable p24 at any time point (data not shown). Furthermore, proviral integrated DNA load was measured at day seven after stimulation in the presence of IRS661 or a control sequence (Fig. 8e) and after transduction with TLR7-specific shRNA (Fig. 8f) to monitor the cellular viral reservoir. Inhibition of TLR7 by either IRS661 or protein knockdown resulted in a highly significant decrease in proviral DNA load as compared to control cells. Taken together these results show that inhibition of TLR7 signaling can reduce HIV-1 load in infected $CD4^+$ T cells derived from infected patients.

Discussion

Microbial pattern recognition receptors are critical for early sensing of diverse bacterial and viral infections activating the innate immune system. Here, we describe a previously unknown function of these pattern recognition receptors in shutting off human $CD4^+$ T cell immune responses. TLR7 ligand engagement in $CD4^+$ T cells prevented entry into cell cycle and proinflammatory cytokine secretion after stimulation. Mechanistically, TLR7 stimulation increased intracellular calcium concentrations that led to NFATc2 dephosphorylation and translocation to the cell nucleus, activating an anergic gene expression program. Furthermore, TLR7 signaling interfered with costimulatory signals, as JNK and Jun activation were inhibited upon activation in the presence of TLR7 ligands. Our results have potential clinical implications, as TLR7 silencing inhibited the frequency of *in vitro* HIV-1-infected cells, and the phenotype of those infected did not display an anergic phenotype, suggesting that the calcium-induced TLR7-dependent anergic state in HIV-1 infected cells could play a role in HIV-1 persistence.

TLR signaling has been predominantly studied in APC where engagement of the ligand induces proinflammatory cytokine secretion and upregulation of activation molecules[12, 13, 14]. Although TLR signaling in $CD4^+$ T cells has not been studied in depth, the few reports published demonstrate a positive costimulatory role for TLR signaling[7, 8, 40]. Our results demonstrate a previously undescribed TLR signaling pathway that has an inhibitory effect on T cell proliferation and cytokine secretion. The differences between the phenotypes observed in monocytes and $CD4^+$ T cells upon TLR7 stimulation could be due to the intrinsic differences in activation requirements for each cell population. Although $CD4^+$ T cells need TCR engagement and a costimulatory signal in order to enter cell cycle stimulated, $CD14^+$ cells require one signal. Thus TLR7 ligand engagement is sufficient to induce activation and proinflammatory cytokine secretion in monocytes, as expected for an innate immune cell. In contrast, TLR7 stimulation in $CD4^+$ T cells leads to a significant increase in intracellular calcium that in the absence of a costimulatory signal triggers the TLR7-driven anergic program[17]. In this respect, our results also show a decrease in $CD4^+$ T cell proliferation upon TLR9 stimulation, with no effect on IFN-γ secretion and a trend towards increased IL-17 secretion, although this is not statistically significant. Furthermore, there is no increase in the intracellular calcium concentration when $CD4^+$ T cells are

stimulated with CpG B, suggesting that the mechanism by which CpG B modifies $CD4^+$ T cell functionality is not common to TLR7 ligation.

It is important to note that all ligands used in this manuscript were pharmacological TLR7 agonists. In this respect, we have not been able to find any immunostimulatory RNA specific for human TLR7, which would be a more physiological ligand, as these sequences were described in mice and they recognize human TLR8 instead. This issue has been overcome by the use of HIV-1 as a potential TLR7 'natural' ligand. The physiological relevance of our data is suggested by the effect TLR7 signaling has on HIV-1 infected cells. Several reports have recently highlighted the role of innate sensors on HIV-1 infection, predominantly focused on the function of these molecules in $CD4^+$ T cells that had not been productively infected[41, 42]. Our results add a new layer of complexity to our understanding of the HIV viral life cycle that needs further investigation and are in contrast with recent published data that describes the cytoplasmic sensors of viral DNA that trigger cell death by pyroptosis of non-productively infected $CD4^+$ T cells[41, 42]. Moreover, the observations reported here suggest the involvement of TLR7 on both induction of the anergic phenotype observed in HIV-1-infected cells and on increases in the degree of $CD4^+$ T cell infection suggesting that TLR7-induced calcium upregulation is involved in virus life cycle. In this regard, TLR8-dependent NF-κB activation has been shown to be critical for HIV-1 replication in DC[43]. Although we have not examined the role of TLR8 on $CD4^+$ T cell infection by HIV-1, it is possible that contribution of both TLR7-driven NF-κB activation and TLR7-induced anergy play a role in the increased viral loads. The observation that anergy favors HIV-1 infection is somewhat paradoxical based on the existing literature showing that HIV-1 infection is favored in activated $CD4^+$ T cells[11]. In this respect, we could speculate that HIV-1 would trigger TLR7 mainly to induce an increase in intracellular calcium concentrations, which has been suggested to be important for the virus life cycle[37]. Whether anergy induction on host cells by HIV-1 infection through TLR7 is a bystander consequence of the increase in intracellular calcium driven by TLR7, and whether this status is beneficial or not for the host is currently unknown. But these observations open up a new field of investigation related to the mechanism, kinetics, and consequences of the interaction of HIV-1 with the host cell through TLR7.

Infections are generally regarded as illness, mammals are colonized with bacteria and viruses. The prime example is that of bacteria adopted for digestion, though humans are also colonized with common DNA and RNA viruses including endogenous retroviruses. It has been suggested that these endogenous retroviruses provide an adoptive selective advantage in generating genetic diversity (for review[44]). Based on our data here we could speculate that TLR7 was co-opted in human $CD4^+$ T cells to co-evolve such that they did not enter into cell cycle in response to endogenous retroviruses with potential consequences such as leukemia (HTLV-1) and autoimmune diseases. In this respect, there are examples in the literature that certain endogenous retrovirus sequences are upregulated in human autoimmune diseases[45]. Although it will be of interest in future investigations to precisely understand when TLR7 is engaged in the HIV-1 infection life-cycle, these data demonstrate a novel mechanism by which HIV-1 may avoid elimination by co-opting NFAT-dependent TLR7-induced T cell anergy.

In summary, we provide a novel role for TLR7 in $CD4^+$ T cell function that is in direct opposition to its role in innate immune cells. Moreover, TLR7 ligands may be used as a means of inducing 'tolerance' on $CD4^+$ T cells in human autoimmune diseases. Finally, these data demonstrate a previously unknown function for microbial pattern recognition receptors in the inhibition of immune responses.

Methods

Cell culture reagents and antibodies

Cells were cultured in RPMI 1640 media supplemented with 2 nM L-glutamine, 5 mM HEPES, and 100 U/μg/ml penicillin/streptomycin (Biowhittaker, Walkersville, MD), 0.5 mM sodium pyruvate, 0.05 mM nonessential amino acids (Life Technologies, Rockville, MD), and 5% human AB serum (Gemini Bio-Products, Woodland, CA). The antibodies used for stimulation were anti-human CD3 (clone UCHT1 and clone Hit3a) and anti-human CD28 (clone 28.2) (BD Biosciences, San Jose, CA) at 1μg/ml. The TLR7 antibody used for staining was from R&D (clone 533707). IL-2 was obtained through the AIDS Research and Reference Reagent Program, Division of AIDS, National Institute of Allergy and Infectious Diseases (NIAID), National Institutes of Health (NIH), and was used at 10 U/ml at the initiation of cultures. All TLR ligands (EndoFit™, <0.001 EU/μg) were purchased from Invivogen and resuspended in endotoxin-free water as per manufacturer recommendations. Phorbol 12-myristate 13-acetate (PMA) and Ionomycin were purchased from Sigma-Aldrich. IRS661 TLR-specific inhibitory sequence[46] was synthesized by Sigma-Aldrich on a phosphorothioate backbone.

Study subjects

Peripheral blood was drawn from healthy individuals after informed consent and approval by the Institutional Review Board at Yale University.

HIV-1 patients

Peripheral blood was obtained from 9 HIV-1-infected patients after informed consent and approval by the Institutional Review Board at Yale University. Patient information provided in Supplementary Table 1.

Cell isolation and flow sorting of T cell populations

Peripheral blood mononuclear cells (PBMC) were isolated from healthy donors by Ficoll Hypaque gradient centrifugation. Total $CD4^+$ T cells were isolated by negative selection using $CD4^+$ T cell isolation kit (StemCell Technologies, Vancouver, BC) and stained for fluorescence-activated cell sorting (FACS) with the following antibodies: anti-CD45RO (clone UCHL1), CD45RA (clone Hl100), CD25 (clone M-A251) (all from BD Biosciences) and CD127 (clone eBioRDR5) from eBioscience (San Diego, CA). The T_{reg} ($CD4^+CD25^{hi}CD127^{low/neg}$), memory T cell ($CD4^+CD45RA^-$ $CD45RO^+CD25^{low/neg+}$) and naive T cell ($CD4^+CD45RA^+CD45RO^-CD25^{lo/neg}$) populations were sorted on a FACS Aria (BD Biosciences). Unless specified, $CD4^+$ T cells used in the experiments were T_{reg}-depleted $CD4^+$ T cells and they were sorted as $CD4^+CD25^{pos/lo}CD127^+$. $CD14^+$ cells were

isolated by positive selection using EasySep™ Human CD14 Positive Selection Kit (StemCell Technologies).

Cell activation and intracellular staining

T cell populations were stimulated with 1 μg/ml anti-CD3, 1 μg/ml anti-CD28 and 10 U/ml IL-2 in the presence or absence of the following TLR ligands (all from Invivogen): Pam3CSK4 (0.5 μg/ml), heat-killed *Listeria monocytogenes* (HKLM, 5×10^7 cells/ml) Poly (I:C) (high molecular weight, 10 μg/ml), ultrapure lipopolysaccharide from *E. coli* K12 strain (10 μg/ml), recombinant flagellin from *Salmonella enterica* (0.2 μg/ml), synthetic diacylated lipoprotein (FSL-1, 0.2 μg/ml), Imiquimod (IMQ, 0.1–10 μg/ml), Gardiquimod (GDQ, 5 μg/ml), Loxoribine (1 mM), CL264 (20 μg/ml), ssRNA40/LyoVec™ (0.5 μg/ml) and ODN2006 (2.5 μM). At day 4, cells were stimulated with 50 ng/ml phorbol-12-myristate-13-acetate (PMA) and 250 ng/ml ionomycin for 4 hours in the presence of GolgiStop (BD Biosciences) and intracellular staining of cytokines (IFN-γ, IL-10, IL-17, IL-4, IL-2) and Foxp3 was performed with Foxp3 staining buffers (eBioscience) per manufacturer´s recommendations and the following antibodies: IFN-γ (clone 4S.B3) and IL-17 (clone BL168) from Biolegend (San Diego, CA), IL-10 (clone JES3-19F1), IFN-γ (clone B27) and IL-4 (clone 3010.211), from BD Biosciences and Foxp3 (clone PCH101) from eBioscience. For both extracellular and intracellular stainings, LIVE/DEAD® reagent (Molecular Probes) was used to exclude dead cells before surface staining. $CD14^+$ monocytes were cultured with different TLR ligands for 24 hours and cell surface staining was performed as described above with an initial FcR blocking step (FcR blocking reagent, human, Miltenyi Biotech). Samples were run on a BD Fortessa instrument and analyzed with FlowJo (TreeStar).

Enzyme-linked immunosorbent assay

ELISA measurement of IFN-γ, IL-2, IL-17, IL-4 and IL-10 from stimulated $CD4^+$ T cell culture supernatants and TNFα, IL-1β and IL-6 from $CD14^+$ cultures was performed according to manufacturer's recommendations. IL-2, IL-17 and IL-10 antibody pairs were obtained from R&D, anti-IFN-γ monoclonal antibody (mAb) (clone 2G1) and human IFN-γ mAb biotin-labeled were from Thermo Scientific, (Rockford, IL) and IL-10, IL-6, TNFα and IL-1β antibody pairs were obtained from BD Biosciences.

Quantification of mRNA expression levels by RT-PCR

RNA was isolated using QIAGEN RNeasy Micro Plus Kit (QIAGEN, Valencia, CA), following manufacturer´s guidelines and converted to cDNA by reverse transcription (RT) with random hexamers and Multiscribe RT (TQMN, Reverse Transcription Reagents; Applied Biosystems, Foster City, CA). For mRNA gene expression assays, the following probes were purchased from Applied Biosystems: *CBLB* (Hs00180288_m1), *DGKA* (Hs00176278_m1), *EGR2* (Hs00166165_m1), *EGR3* (Hs00231780_m1), *NFATC2* (Hs00234855_m1), *SIRT1* (Hs01009003_m1), *ITCH* (Hs00395201_m1), *IL17A* (Hs00936345_m1), *IL4* (Hs00929862_m1), *IFNG* (Hs00989291_m1), *IL10* (Hs00961622_m1), *FOXP3* (Hs01085834_m1), *TBX21* (Hs00203436_m1), *RORC2* (Hs01076112_m1), *GATA3* (Hs00231122_m1), *IL2* (Hs00914135_m1), *TLR7*

(Hs00152971_m1), *TLR8* (Hs00152972_m1), *CASP3* (Hs00991554_m1), *CD98* (Hs00374243_m1), *FASL* (Hs00181225_m1), *GRG4* (Hs00419101_m1), *IKZF1* (Hs00958474_m1), *KMD6B* (Hs00996325_g1), *LDHA* (Hs00855332_g1), *RAB10* (Hs00211643_m1), *RGS2* (Hs01009070_g1), *SOCS2* (Hs00919620_m1), *TNFRSF9* (Hs00155512_m1), *TRAF5* (Hs00182979_m1), *B2M* (4326319E). The reactions were set up following manufacturer´s guidelines and run on a StepOne Real-Time PCR System (Applied Biosystems). Values are represented as the difference in Ct values normalized to β2-microglobulin for each sample as per the following formula: Relative RNA expression = $(2^{-dCt}) \times 1000$.

Immunoblotting

Total protein extracts were isolated with M-PER protein extraction kit (Thermo Scientific) and quantified with a BCA kit (Thermo Scientific). 20μg of protein extract were loaded per lane, separated on a 10% SDS-PAGE gel and transferred to a nitrocellulose membrane. anti-NFAT1 and anti-β-actin were obtained from Cell Signaling Technology. Anti-pNFAT (Ser213/217/229) antibody was obtained from Santa Cruz Biotechnology (Dallas, TX). Primary antibodies were detected by secondary anti-rabbit-HRP-conjugated (Cell Signaling Technology) and images were obtained in a CCD camera instrument. Bands were quantified with QuantityOne software.

Intracellular calcium measurements

Ex vivo isolated $CD4^+$ T cells were labeled with 5μM Indo-1AM for one hour at 37°C in PBS, 1mM Ca^{2+}. Cells were washed to remove traces of Indo-1AM, resuspended in buffer at 10^6 cells/ml and incubated for 30 minutes at 37°C before analysis. When necessary, IRS661 was added at the indicated concentration during the 30 minutes incubation. For acquisition, the sample was acquired for approximately 3 minutes to obtain basal levels of calcium and subsequently IMQ or other reagents were added at the indicated concentrations. Samples were acquired for a minimum of 10 minutes on a BD Fortessa instrument and analysed with FlowJo software.

Gene silencing by lentiviral transduction

Lentiviral particles encoding shRNAs were obtained from Sigma-Aldrich (NFAT1 clone TRCN0000016144, TLR7 clones 3 and 4 TRCN0000056973 and TRCN0000056974, respectively). 5×10^4 $CD4^+$ T cells per well were stimulated with plate-bound anti-CD3 (1μg/ml) and soluble anti-CD28 (1μg/ml) for 12h before transduction. Cells were then transduced with viral particles containing a vector expressing the indicated specific shRNA (NFAT1 or TLR7) or a non-target shRNA as a control at a multiplicity of infection of 4. All constructions contained the coding sequence for GFP. After 5 days in culture, transduced cells were sorted based on GFP expression and the efficiency of gene silencing was determined by TaqMan real-time PCR and protein staining.

Preparation of HIV-1 virus stocks

HIV-1 proviral DsRed-tagged DNA pNL-D (derived from the prototype HIV-1 proviral DNA pNL432) was kindly provided by Dr. Yasuko Tsunetsugu-Yokota. 293T cells were

used to prepare viral stocks following published protocols[35] with minor modifications. In brief, 293T cells were plated at 0.5×10^6/well in 12-well plates and transfected with 2μg pNL-D using Lipofectamine 2000 (Invitrogen) for 48 hours. Culture supernatant was treated with benzonase (1U/ml) for 30 minutes at 37C, cleared by filtration and titrated on 293T cells. Stocks were stored at −80C.

HIV-1 *in vitro* infection

$CD4^+$ T cells were stimulated with anti-CD3 (1 μg/ml) and anti-CD28 (1 μg/ml) for 48 hours and subsequently infected with HIV-1 at a MOI of 0.001 (concentration within the physiological range[34]). Viability and cytokine secretion was measured every 48 hours for a total of 11 days after infection.

For HIV-1 infection on TLR7-deficient cells, $CD4^+$ T cells were stimulated as above and transduced with the corresponding lentiviral particles. 2 days after transduction, the cells were infected with $HIV\text{-}1_{NL\text{-}D}$ at a MOI of 0.001. Viability and frequency of HIV-1-infected cells was measured at different time points by LIVE/DEAD cell dye staining and fixation with 1%PFA. For intracellular staining after infection, the cells were restimulated with PMA and Ionomycin in the presence of GolgiStop for 4 hours and the staining was performed as recommended with the Foxp3 staining kit (eBioscience) with a pre-fixation step with 1% PFA to avoid DsRed signal loss.

DNA proviral load

50×10^3 $CD4^+$ T cells were stimulated as above and DNA was isolated after 7 days for DNA proviral load measurement as previously published[47].

T cell clones

$CD4^+$ T cells were sorted at one cell per well in 96 well plates and stimulated with anti-CD3 (1μg/ml), anti-CD28 (1μg/ml), IL-2 (25 U/ml) and 50000 irradiated T cell-depleted PBMC for 18 days. Media was replaced every 3 days. After 18 days, clones were stimulated with anti-CD3 and anti-CD28 for 3 days in the presence or absence of IMQ, and supernatant was collected for ELISA analysis and cells were lysed for RNA isolation.

Apoptosis staining

$CD4^+$ T cells were stimulated with anti-CD3 (1 μg/ml) and anti-CD28 (1 μg/ml) for 48 hours and subsequently infected with $HIV\text{-}1_{NL\text{-}D}$ at a MOI of 0.001. Annexin V and 7-AAD were used to stain for early (Annexin V^+ 7-AAD^-) and late (7-AAD^+) apoptosis every 24 hours for a total of 11 days.

Analysis of phosphorylation by flow cytometry

$CD4^+$ T cells were stimulated with 10 μg/ml IMQ in the presence or absence of 50 ng/ml PMA and 250 ng/ml Ionomycin and the cells were fixed at different time points with Fixation buffer (BD Biosciences), permeabilized with Perm buffer III following manufacturer's recommendations, and stained with PE-labeled mouse anti-p38 MAPK (pT180/pY182), Alexa Fluor 488-labeled NFκB p65 (pS529), from BD Biosciences and

Alexa Fluor 647-labeled mouse p-JNK (T183/Y185), PE-labeled rabbit p-IRAK4 (T345/S346) and PE-labeled p-cJun (S73), from Cell Signaling.

In vitro anergy induction

$CD4^+$ T cells were incubated with either 1μM Ionomycin or 0.5 μg/ml plate-bound anti-CD3 (or vehicle as a control) for 12 hours, washed and restimulated with anti-CD3 and anti-CD28 after a 6 hour resting period. Two days later, cells were infected with HIV-1, and frequency of infected cells was examined every other day for a total of 11 days.

Statistics

Statistical analysis was performed using GraphPad Prism (GraphPad Software). A standard paired two-tailed *t* test was used for statistical analysis and a one-way ANOVA with a Tukey's post-test for more than two groups comparisons; p values of 0.05 or less were considered significant. Data were presented if not indicated elsewhere as mean±s.e.m. (*p<0.05, **p<0.005, ***p<0.0005).

Supplementary Material

Refer to Web version on PubMed Central for supplementary material.

Acknowledgments

The authors would like to thank Lesley Devine and Zhao Wang for technical assistance, Dr. Yasuko Tsunetsugu-Yokota for kindly providing the HIV-1_{NL-D} proviral DNA, Dr. Douglas Bruce, Dr. Heidi Zapata and Dr. Betsy Clement Herold and her laboratory for patient recruitment and Hafler lab members for helpful comments and suggestions.

This work was supported by a National MS Society Collaborative Research Center Award CA1061-A-18, National Institutes of Health Grants P01 AI045757, U19 AI046130, U19 AI070352, P01 AI039671 (to D.A.H.) and R01 AI065309 (to M.J.K.), the Penates Foundation and the Nancy Taylor Foundation for Chronic Diseases, Inc. (to D.A.H.), and a Nancy Davis Junior Investigator Award (to M.D.V.)

References

1. Song DH, Lee JO. Sensing of microbial molecular patterns by Toll-like receptors. Immunological reviews. 2012; 250(1):216–229. [PubMed: 23046132]
2. Diebold SS, Kaisho T, Hemmi H, Akira S, Reis e Sousa C. Innate antiviral responses by means of TLR7-mediated recognition of single-stranded RNA. Science. 2004; 303(5663):1529–1531. [PubMed: 14976261]
3. Heil F, Hemmi H, Hochrein H, Ampenberger F, Kirschning C, Akira S, et al. Species-specific recognition of single-stranded RNA via toll-like receptor 7 and 8. Science. 2004; 303(5663):1526–1529. [PubMed: 14976262]
4. Kugelberg E. Innate immunity: Making mice more human the TLR8 way. Nature reviews Immunology. 2014; 14(1):6.
5. Kawai T, Akira S. Innate immune recognition of viral infection. Nature immunology. 2006; 7(2): 131–137. [PubMed: 16424890]
6. Kabelitz D. Expression and function of Toll-like receptors in T lymphocytes. Current opinion in immunology. 2007; 19(1):39–45. [PubMed: 17129718]
7. Gelman AE, Zhang J, Choi Y, Turka LA. Toll-like receptor ligands directly promote activated CD4+ T cell survival. J Immunol. 2004; 172(10):6065–6073. [PubMed: 15128790]

8. Caron G, Duluc D, Fremaux I, Jeannin P, David C, Gascan H, et al. Direct stimulation of human T cells via TLR5 and TLR7/8: flagellin and R-848 up-regulate proliferation and IFN-gamma production by memory CD4+ T cells. J Immunol. 2005; 175(3):1551–1557. [PubMed: 16034093]
9. Grakoui A, Shoukry NH, Woollard DJ, Han JH, Hanson HL, Ghrayeb J, et al. HCV persistence and immune evasion in the absence of memory T cell help. Science. 2003; 302(5645):659–662. [PubMed: 14576438]
10. Lechner F, Wong DK, Dunbar PR, Chapman R, Chung RT, Dohrenwend P, et al. Analysis of successful immune responses in persons infected with hepatitis C virus. The Journal of experimental medicine. 2000; 191(9):1499–1512. [PubMed: 10790425]
11. Walker B, McMichael A. The T-Cell Response to HIV. Cold Spring Harbor Perspectives in Medicine. 2012; 2(11)
12. Chamberlain ND, Kim SJ, Vila OM, Volin MV, Volkov S, Pope RM, et al. Ligation of TLR7 by rheumatoid arthritis synovial fluid single strand RNA induces transcription of TNFalpha in monocytes. Annals of the rheumatic diseases. 2013; 72(3):418–426. [PubMed: 22730373]
13. Cros J, Cagnard N, Woollard K, Patey N, Zhang SY, Senechal B, et al. Human CD14dim monocytes patrol and sense nucleic acids and viruses via TLR7 and TLR8 receptors. Immunity. 2010; 33(3):375–386. [PubMed: 20832340]
14. Dzopalic T, Dragicevic A, Vasilijic S, Vucevic D, Majstorovic I, Bozic B, et al. Loxoribine, a selective Toll-like receptor 7 agonist, induces maturation of human monocyte-derived dendritic cells and stimulates their Th-1- and Th-17-polarizing capability. International immunopharmacology. 2010; 10(11):1428–1433. [PubMed: 20817120]
15. Chappert P, Schwartz RH. Induction of T cell anergy: integration of environmental cues and infectious tolerance. Current opinion in immunology. 2010; 22(5):552–559. [PubMed: 20869863]
16. Quill H, Schwartz RH. Stimulation of normal inducer T cell clones with antigen presented by purified Ia molecules in planar lipid membranes: specific induction of a long-lived state of proliferative nonresponsiveness. J Immunol. 1987; 138(11):3704–3712. [PubMed: 3035012]
17. Macian F, Garcia-Cozar F, Im SH, Horton HF, Byrne MC, Rao A. Transcriptional mechanisms underlying lymphocyte tolerance. Cell. 2002; 109(6):719–731. [PubMed: 12086671]
18. Lenert PS. Classification, mechanisms of action, and therapeutic applications of inhibitory oligonucleotides for Toll-like receptors (TLR) 7 and 9. Mediators of inflammation. 2010; 2010:986596. [PubMed: 20490286]
19. Schwartz RH. Models of T cell anergy: is there a common molecular mechanism? The Journal of experimental medicine. 1996; 184(1):1–8. [PubMed: 8691122]
20. Luo C, Burgeon E, Carew JA, McCaffrey PG, Badalian TM, Lane WS, et al. Recombinant NFAT1 (NFATp) is regulated by calcineurin in T cells and mediates transcription of several cytokine genes. Molecular and cellular biology. 1996; 16(7):3955–3966. [PubMed: 8668213]
21. Luo C, Shaw KT, Raghavan A, Aramburu J, Garcia-Cozar F, Perrino BA, et al. Interaction of calcineurin with a domain of the transcription factor NFAT1 that controls nuclear import. Proceedings of the National Academy of Sciences of the United States of America. 1996; 93(17): 8907–8912. [PubMed: 8799126]
22. Okamura H, Aramburu J, Garcia-Rodriguez C, Viola JP, Raghavan A, Tahiliani M, et al. Concerted dephosphorylation of the transcription factor NFAT1 induces a conformational switch that regulates transcriptional activity. Molecular cell. 2000; 6(3):539–550. [PubMed: 11030334]
23. Gao B, Kong Q, Kemp K, Zhao YS, Fang D. Analysis of sirtuin 1 expression reveals a molecular explanation of IL-2-mediated reversal of T-cell tolerance. Proceedings of the National Academy of Sciences of the United States of America. 2012; 109(3):899–904. [PubMed: 22219356]
24. Heissmeyer V, Macian F, Im SH, Varma R, Feske S, Venuprasad K, et al. Calcineurin imposes T cell unresponsiveness through targeted proteolysis of signaling proteins. Nature immunology. 2004; 5(3):255–265. [PubMed: 14973438]
25. Jeon MS, Atfield A, Venuprasad K, Krawczyk C, Sarao R, Elly C, et al. Essential role of the E3 ubiquitin ligase Cbl-b in T cell anergy induction. Immunity. 2004; 21(2):167–177. [PubMed: 15308098]

26. Zha Y, Marks R, Ho AW, Peterson AC, Janardhan S, Brown I, et al. T cell anergy is reversed by active Ras and is regulated by diacylglycerol kinase-alpha. Nature immunology. 2006; 7(11): 1166–1173. [PubMed: 17028589]
27. Safford M, Collins S, Lutz MA, Allen A, Huang CT, Kowalski J, et al. Egr-2 and Egr-3 are negative regulators of T cell activation. Nature immunology. 2005; 6(5):472–480. [PubMed: 15834410]
28. Castellanos MC, Munoz C, Montoya MC, Lara-Pezzi E, Lopez-Cabrera M, de Landazuri MO. Expression of the leukocyte early activation antigen CD69 is regulated by the transcription factor AP-1. J Immunol. 1997; 159(11):5463–5473. [PubMed: 9580241]
29. Kim JO, Kim HW, Baek KM, Kang CY. NF-kappaB and AP-1 regulate activation-dependent CD137 (4-1BB) expression in T cells. FEBS letters. 2003; 541(1–3):163–170. [PubMed: 12706838]
30. Miedema F. Immunological abnormalities in the natural history of HIV infection: mechanisms and clinical relevance. Immunodeficiency reviews. 1992; 3(3):173–193. [PubMed: 1354968]
31. Faith A, O'Hehir RE, Malkovsky M, Lamb JR. Analysis of the basis of resistance and susceptibility of CD4+ T cells to human immunodeficiency virus (HIV)-gp120 induced anergy. Immunology. 1992; 76(2):177–184. [PubMed: 1353060]
32. Cayota A, Vuillier F, Gonzalez G, Dighiero G. In vitro antioxidant treatment recovers proliferative responses of anergic CD4+ lymphocytes from human immunodeficiency virus-infected individuals. Blood. 1996; 87(11):4746–4753. [PubMed: 8639845]
33. Maggi E, Macchia D, Parronchi P, Mazzetti M, Ravina A, Milo D, et al. Reduced production of interleukin 2 and interferon-gamma and enhanced helper activity for IgG synthesis by cloned CD4+ T cells from patients with AIDS. European journal of immunology. 1987; 17(12):1685–1690. [PubMed: 2961571]
34. Chen H, Li C, Huang J, Cung T, Seiss K, Beamon J, et al. CD4+ T cells from elite controllers resist HIV-1 infection by selective upregulation of p21. The Journal of clinical investigation. 2011; 121(4):1549–1560. [PubMed: 21403397]
35. Yamamoto T, Tsunetsugu-Yokota Y, Mitsuki YY, Mizukoshi F, Tsuchiya T, Terahara K, et al. Selective transmission of R5 HIV-1 over X4 HIV-1 at the dendritic cell-T cell infectious synapse is determined by the T cell activation state. PLoS pathogens. 2009; 5(1):e1000279. [PubMed: 19180188]
36. Bigby M, Wang P, Fierro JF, Sy MS. Phorbol myristate acetate-induced down-modulation of CD4 is dependent on calmodulin and intracellular calcium. J Immunol. 1990; 144(8):3111–3116. [PubMed: 2109010]
37. Cloyd MW, Lynn WS, Ramsey K, Baron S. Inhibition of human immunodeficiency virus (HIV-1) infection by diphenylhydantoin (dilantin) implicates role of cellular calcium in virus life cycle. Virology. 1989; 173(2):581–590. [PubMed: 2574518]
38. Aramburu J, Yaffe MB, Lopez-Rodriguez C, Cantley LC, Hogan PG, Rao A. Affinity-driven peptide selection of an NFAT inhibitor more selective than cyclosporin A. Science. 1999; 285(5436):2129–2133. [PubMed: 10497131]
39. Kinoshita S, Su L, Amano M, Timmerman LA, Kaneshima H, Nolan GP. The T cell activation factor NF-ATc positively regulates HIV-1 replication and gene expression in T cells. Immunity. 1997; 6(3):235–244. [PubMed: 9075924]
40. Crellin NK, Garcia RV, Hadisfar O, Allan SE, Steiner TS, Levings MK. Human CD4+ T cells express TLR5 and its ligand flagellin enhances the suppressive capacity and expression of FOXP3 in CD4+CD25+ T regulatory cells. J Immunol. 2005; 175(12):8051–8059. [PubMed: 16339542]
41. Monroe KM, Yang Z, Johnson JR, Geng X, Doitsh G, Krogan NJ, et al. IFI16 DNA sensor is required for death of lymphoid CD4 T cells abortively infected with HIV. Science. 2014; 343(6169):428–432. [PubMed: 24356113]
42. Yan N, Regalado-Magdos AD, Stiggelbout B, Lee-Kirsch MA, Lieberman J. The cytosolic exonuclease TREX1 inhibits the innate immune response to human immunodeficiency virus type 1. Nature immunology. 2010; 11(11):1005–1013. [PubMed: 20871604]

43. Gringhuis SI, van der Vlist M, van den Berg LM, den Dunnen J, Litjens M, Geijtenbeek TB. HIV-1 exploits innate signaling by TLR8 and DC-SIGN for productive infection of dendritic cells. Nature immunology. 2010; 11(5):419–426. [PubMed: 20364151]

44. de la Casa-Esperon E. Horizontal transfer and the evolution of host-pathogen interactions. International journal of evolutionary biology. 2012; 2012:679045. [PubMed: 23227424]

45. Balada E, Vilardell-Tarres M, Ordi-Ros J. Implication of human endogenous retroviruses in the development of autoimmune diseases. International reviews of immunology. 2010; 29(4):351–370. [PubMed: 20635879]

46. Pawar RD, Ramanjaneyulu A, Kulkarni OP, Lech M, Segerer S, Anders HJ. Inhibition of Toll-like receptor-7 (TLR-7) or TLR-7 plus TLR-9 attenuates glomerulonephritis and lung injury in experimental lupus. Journal of the American Society of Nephrology : JASN. 2007; 18(6):1721–1731. [PubMed: 17460144]

47. Gibellini D, Vitone F, Schiavone P, Ponti C, La Placa M, Re MC. Quantitative detection of human immunodeficiency virus type 1 (HIV-1) proviral DNA in peripheral blood mononuclear cells by SYBR green real-time PCR technique. Journal of clinical virology : the official publication of the Pan American Society for Clinical Virology. 2004; 29(4):282–289. [PubMed: 15018857]

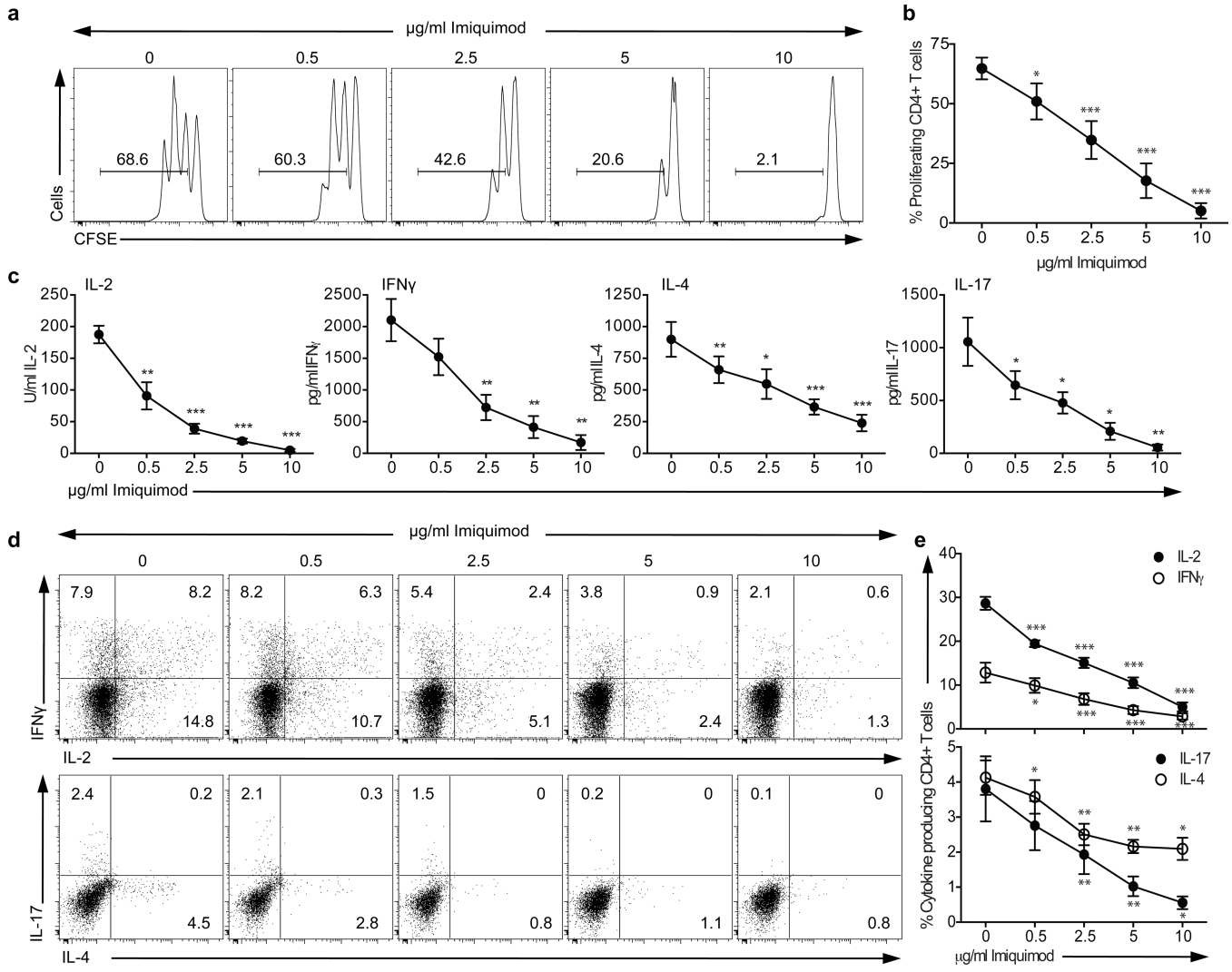

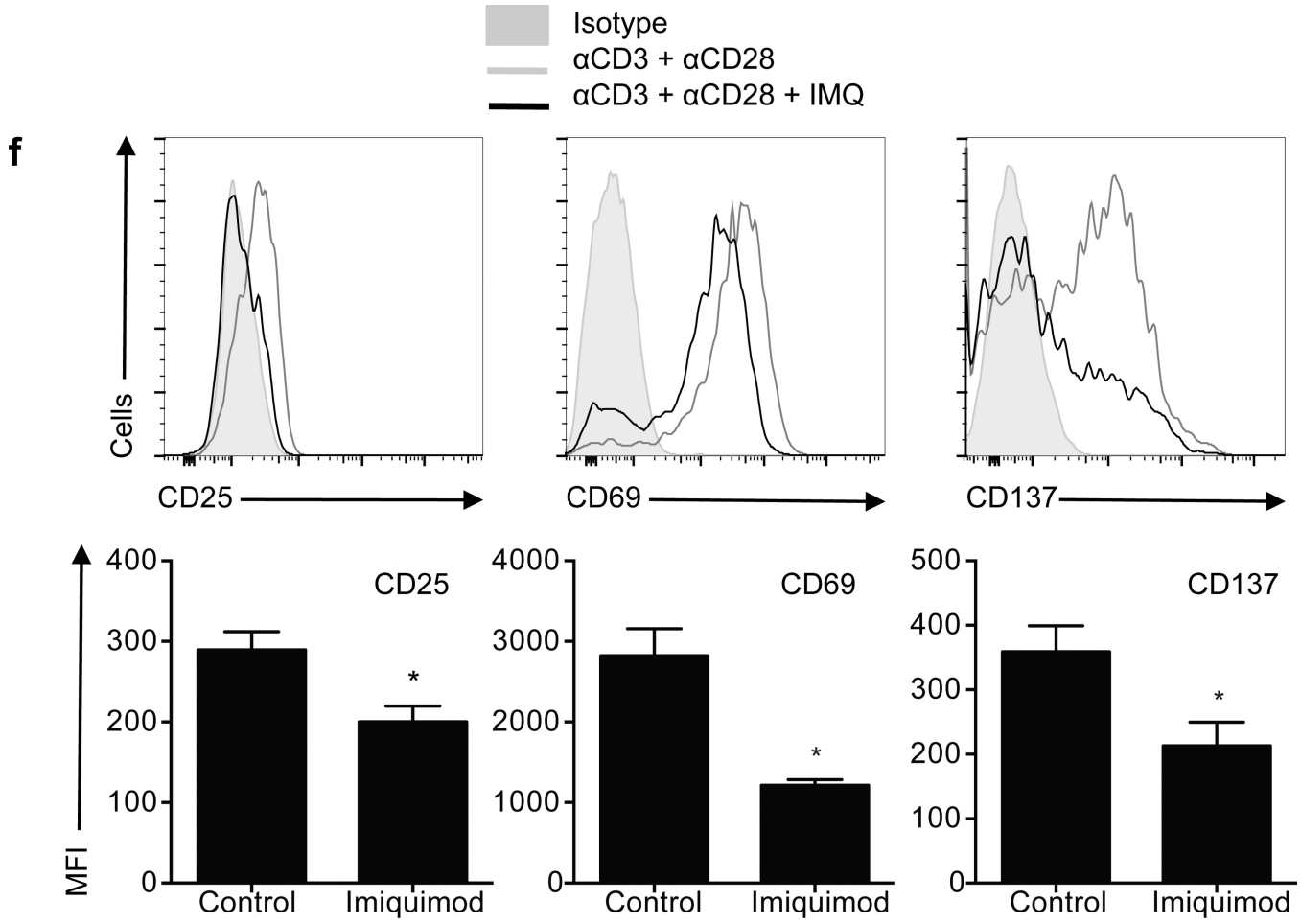

Figure 1.

TLR7 signaling inhibits proliferation and cytokine secretion on $CD4^+$ T cells. $CD4^+$ T cells were stimulated for four days in the presence of different concentrations of Imiquimod (IMQ). **a**. Histograms show CFSE-labeled $CD4^+$ T cell proliferation after 3 days of stimulation. Numbers in histograms represent the frequency of viable proliferating $CD4^+$ T cells. **b**. Frequency of viable proliferating $CD4^+$ T cells stimulated in the presence of different concentrations of IMQ. **c**. Cytokine secretion measured by ELISA after 3 days. **d**. Intracellular staining after a 4 hour PMA and ionomycin stimulation at day four. **e**. Frequency of cytokine-producing $CD4^+$ T cells. **f.** Representative example of the expression (upper row) and MFI (lower row) of CD25 (left), CD69 (middle) and CD137 (right panel) on stimulated cells in the presence (black open histogram) or absence (gray open histogram) of IMQ as compared to isotype control (gray curve). Statistical analyses represent mean± s.e.m. of eight independent experiments with one donor each, performed for **a** and **c**, and six independent experiments with one donor each for **e** and **f**. * $p<0.05$, ** $p<0.005$, *** $p<0.0005$.

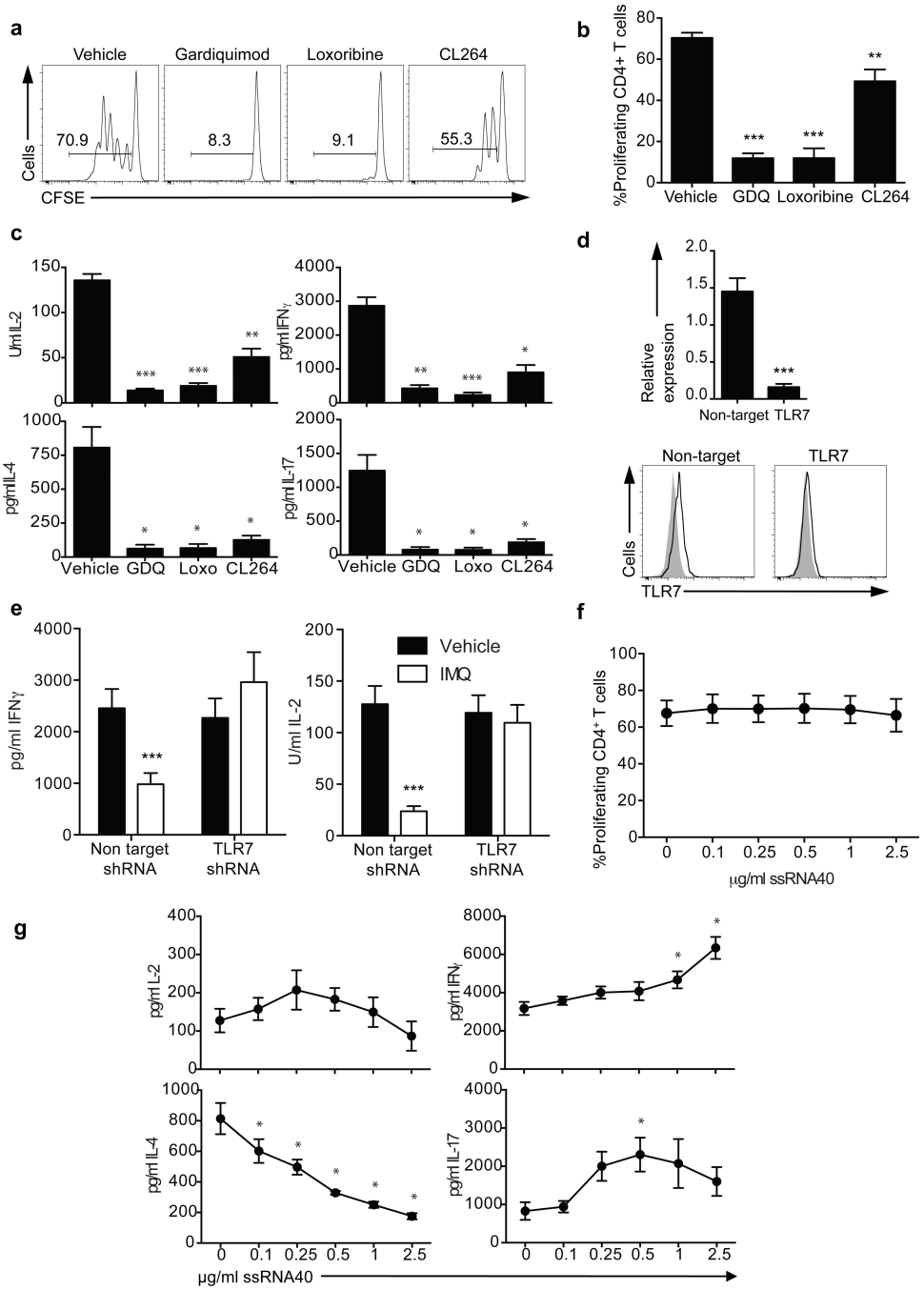

Figure 2.

The inhibitory effect of IMQ is TLR7-specific. CD4$^+$ T cells were stimulated for 3 days in the presence of the TLR7 agonists GDQ, Loxoribine and CL264. **a**. Histograms show CFSE-labeled CD4$^+$ T cell proliferation 3 days after stimulation. Numbers in histograms represent the frequency of viable proliferating CD4$^+$ T cells. **b**. Frequency of viable proliferating CD4$^+$ T cells. **c**. Cytokine secretion measured by ELISA after 3 days. **d**. CD4$^+$ T cells were stimulated in the presence of a shRNA specific for TLR7 (clone TRCN0000056973) or a non-target control. Transduced cells were sorted based on GFP

expression at day 5 and TLR7 RNA (upper) and protein (lower) expression were examined. Histograms represent isotype control (gray histograms) and TLR7 (open histograms). **e**. Non-target and TLR7 shRNA-transduced $CD4^+$ T cells were stimulated in the presence (white bars) or absence (black bars) of IMQ for 3 days and IL-2 and IFN-γ secretion was measured by ELISA. **f.** CFSE-labeled $CD4^+$ T cells were stimulated with anti-CD3 and anti-CD28 in the presence of different doses of ssRNA40. Statistical analysis of the frequency of proliferating $CD4^+$ T cells with increasing concentrations of ssRNA40 (n=4 donors in 4 independent experiments). **g**. IL-2, IFN-γ, IL-4 and IL-17 secretion measured at day 3 after activation by ELISA (n=4 donors in 4 independent experiments). Statistical analysis represents mean±s.e.m. of seven independent experiments performed for a, b, d and e, five experiments for c and four experiments for f and g. * $p<0.05$, ** $p<0.005$, *** $p<0.0005$.

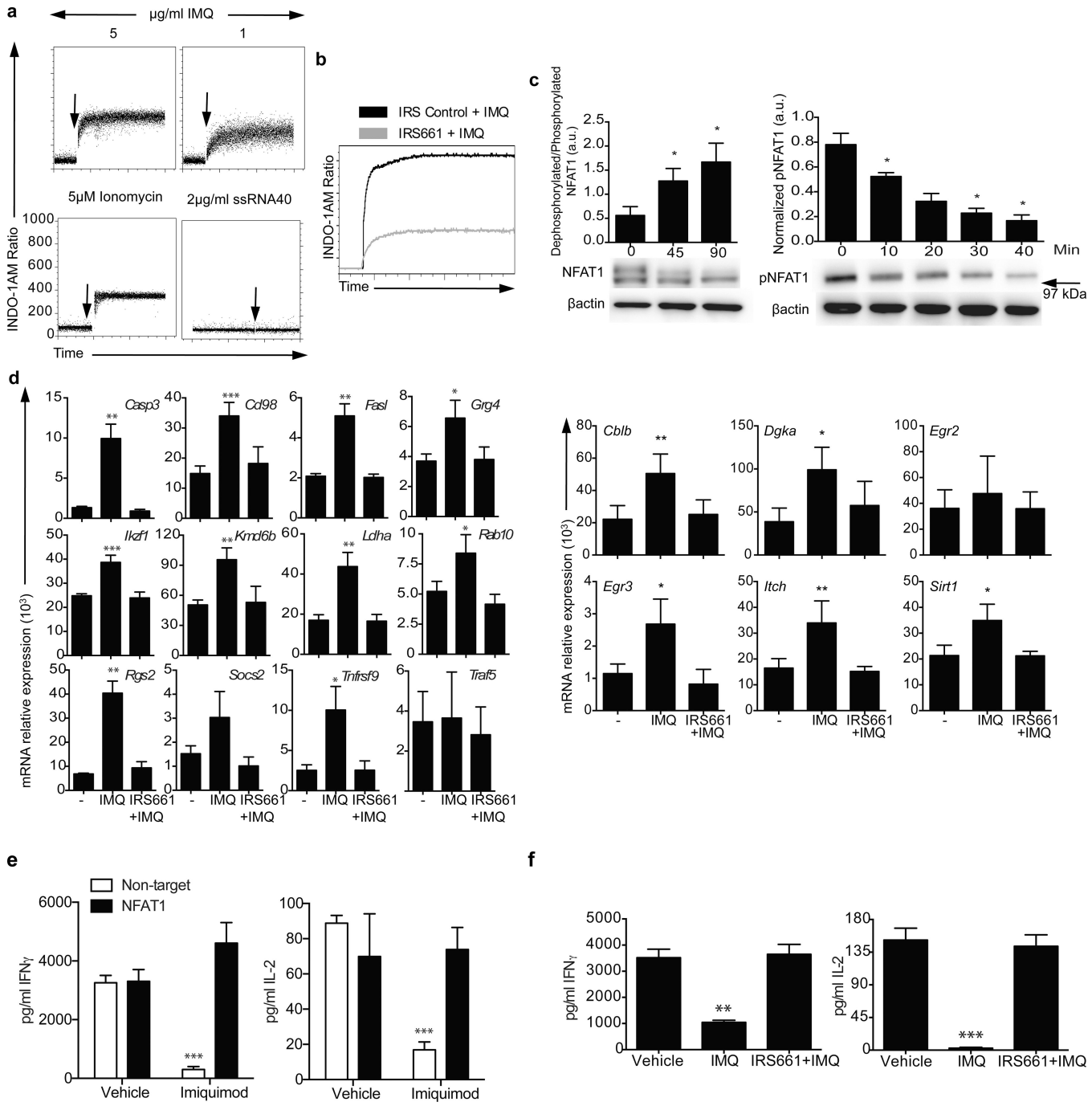

Figure 3.

Mechanism of TLR7-induced anergy. **a**. Plots represent calcium fluxes as measured by Indo-1AM ratio over time in CD4$^+$ T cells stimulated with two concentrations of IMQ (upper), ionomycin (lower left) or ssRNA40-LyoVec™ (lower right). Arrows indicate the addition of IMQ. **b**. Calcium flux in CD4$^+$ T cells pre-incubated for one hour with a control sequence (black) or a specific TLR7 inhibitory sequence (10 μM IRS661, gray) and stimulated with 5 μg/ml IMQ. **c**. Dephosphorylated/phosphorylated NFAT1 ratio at 0, 45 and 90 minutes after IMQ treatment as measured by immunoblot with an anti-NFAT1

antibody (below). Bar charts represent normalized phospho-NFAT intensity at 0, 10, 20, 30 and 40 minutes after stimulation with IMQ. **d**. Anergy-related genes expression on $CD4^+$ T cells stimulated with vehicle, IMQ or IRS661+IMQ for 2 hours. **e**. Non-target (white bars) and NFAT1 (black bars) shRNA-transduced $CD4^+$ T cells were stimulated in the presence or absence of IMQ for 3 days and IL-2 and IFN-γ secretion was measured by ELISA. **f**. $CD4^+$ T cells were incubated with vehicle and IMQ in the presence or absence or IRS661 for two hours, washed and stimulated with anti-CD3 and anti-CD28 for 2 days after a 12 hour resting period. IFN-γ and IL-2 were measured by ELISA. Statistical analysis represents mean±s.e.m. of 6 independent experiments performed for a and b, 5 experiments for c and d, 3 experiments for e and 4 experiments for Fig. f (each experiment with one donor). * $p<0.05$, ** $p<0.005$, *** $p<0.0005$.

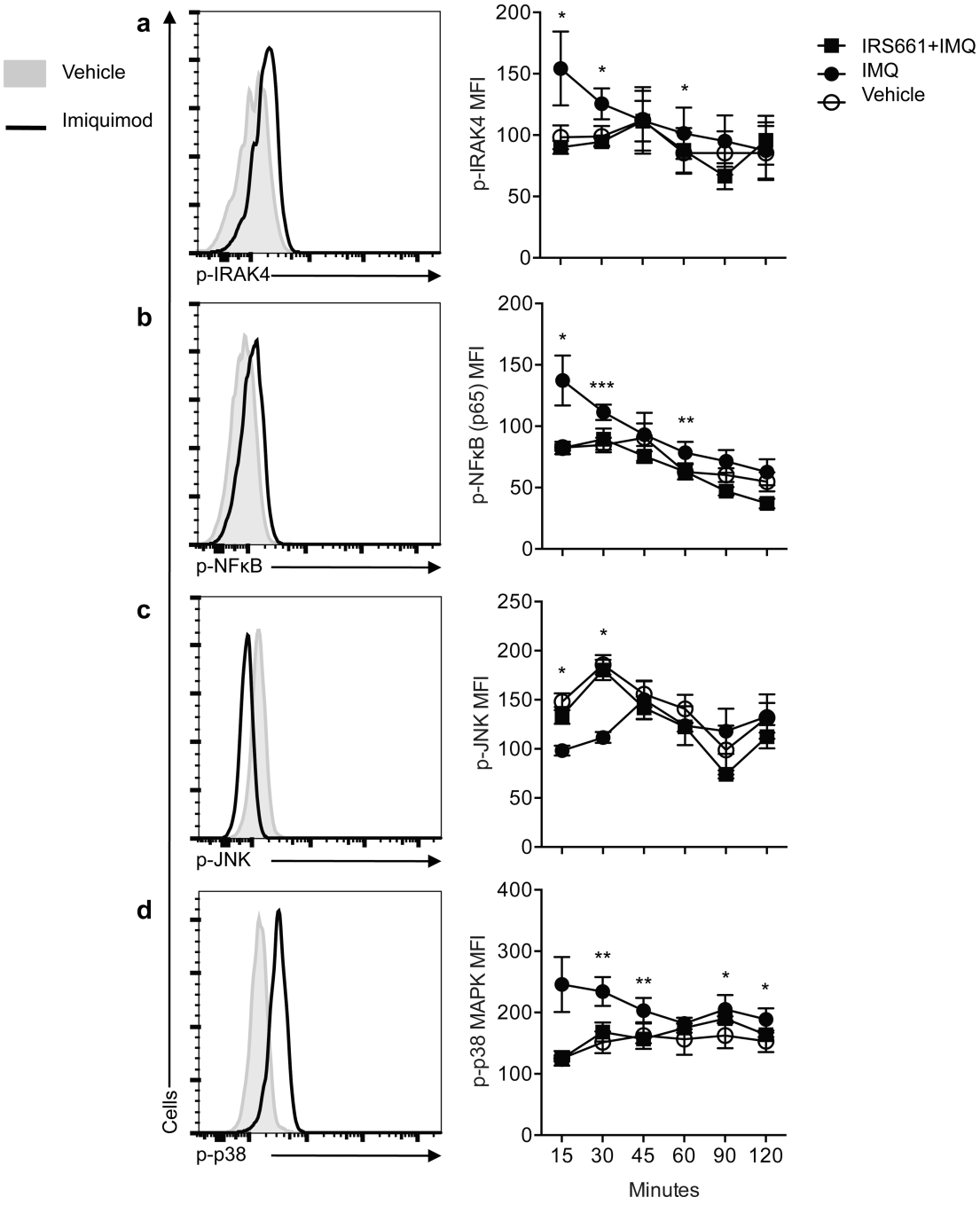

Figure 4. IMQ inhibits JNK phosphorylation

$CD4^+$ T cells were stimulated for 2 hours with IMQ or vehicle. Histograms on the left show a representative example of the expression of the following phosphorylated molecules: IRAK4 (**a**), NF-κB p65 (**b**), JNK (**c**) and p38 (**d**) at 30 minutes after stimulation in vehicle- (gray histogram) or IMQ-treated (dark open histogram) $CD4^+$ T cells. Diagrams on the right show the statistical analysis of 8 independent experiments with one donor each performed. *p<0.05, **p<0.005, ***p<0.0005.

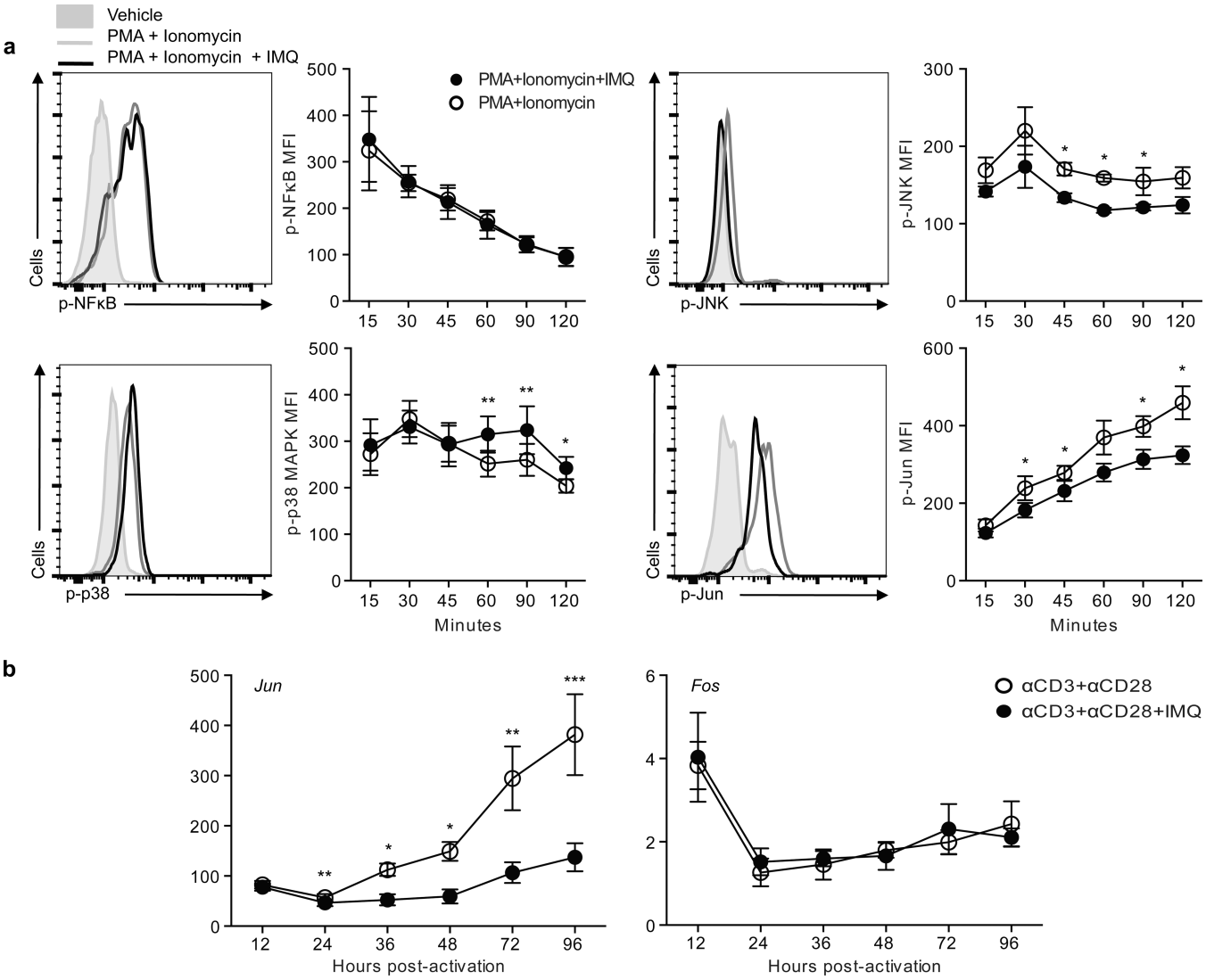

Figure 5.

IMQ inhibits JNK and Jun activation after full CD4$^+$ T cell stimulation. CD4$^+$ T cells were stimulated for 2 hours with PMA and Ionomycin in the presence or absence of IMQ. **a.** Histograms show a representative example of the expression of phosphorylated molecules (NF-κB p65, JNK, p38 cJun) at 60 minutes after activation in PMA+Ionomycin- (gray open histogram) or PMA+Ionomycin+IMQ-treated (dark open histogram) CD4$^+$ T cells as compared to vehicle (gray histogram). Plots show the kinetics analysis of phosphorylation of 8 independent experiments performed with one donor each (right). **b**. Kinetics of *FOS* and *JUN* mRNA gene expression after stimulation of CD4$^+$ T cells in the presence (black) or absence (white) of IMQ, shown as mean±s.e.m. of n=4 donors in 4 independent experiments. *p<0.05, **p<0.005, ***p<0.0005.

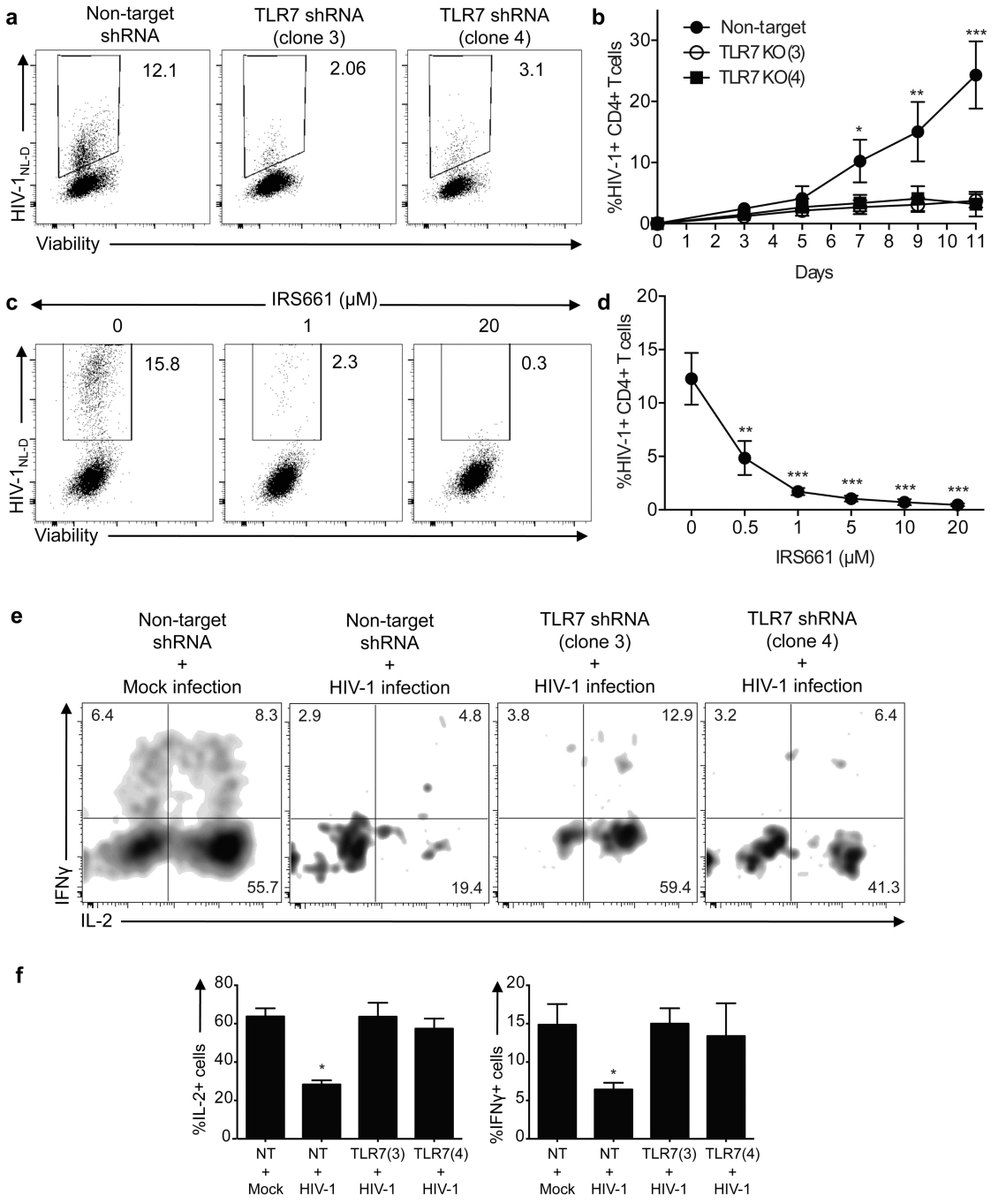

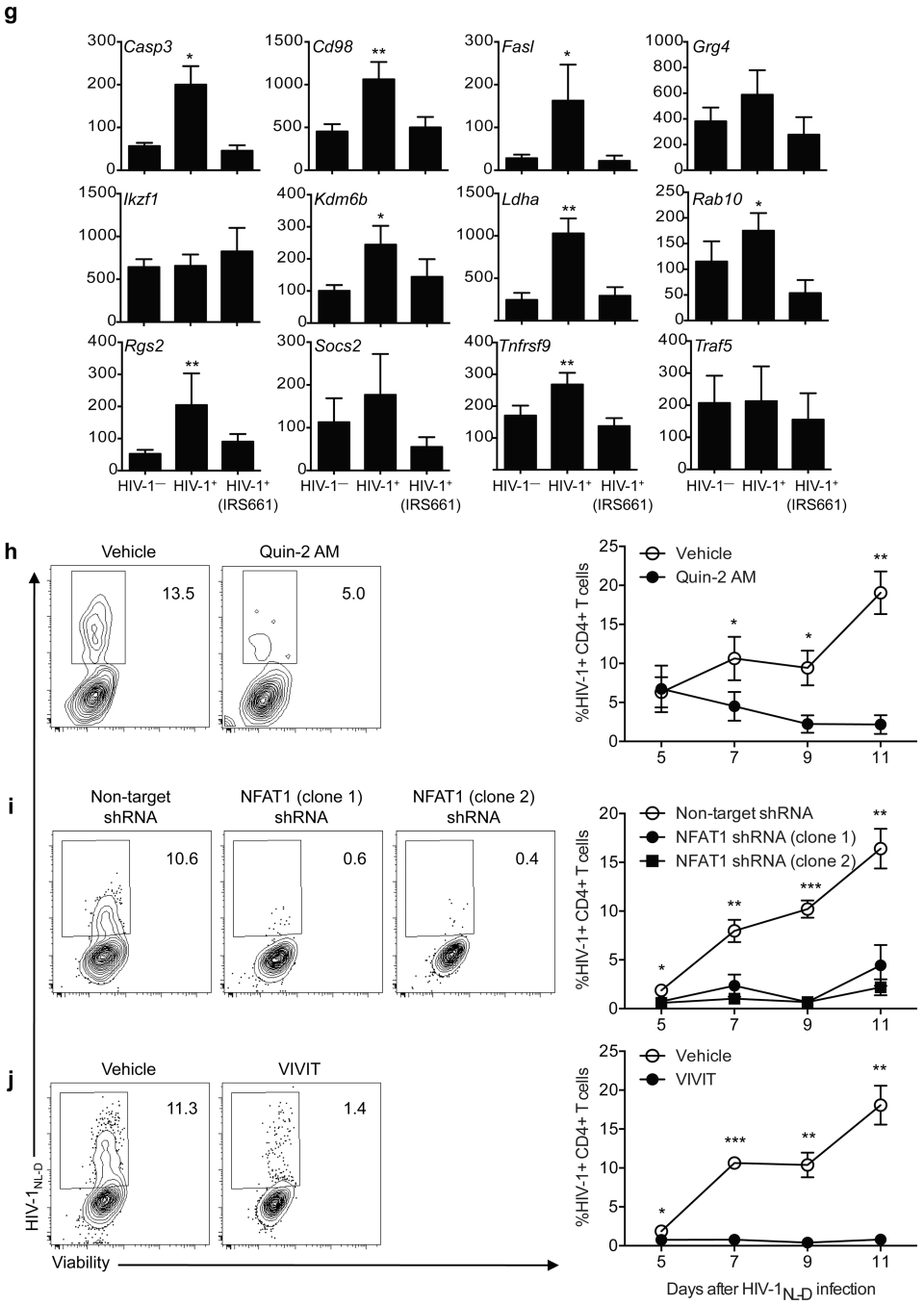

Figure 6.

TLR7 and NFAT knock down abolishes HIV-1 infection. **a**. Dot plots show a representative example of the frequency of viable HIV-1^+ $CD4^+$ T cells on non-target (left dot plot, NT) or TLR7 shRNA-transduced $CD4^+$ T cells (middle and right dot plots, shRNA clones 3 and 4) at day 7 after infection. **b**. Kinetics of HIV-$1_{NL\text{-}D}$ infection on non-target (NT) or TLR7 shRNA-transduced $CD4^+$ T cells (TLR7(3) and TLR7(4)) (n=5 donors in 5 independent experiments). **c**. Dot plots show a representative example of the frequency of viable HIV-1^+ $CD4^+$ T cells stimulated in the presence of various doses of IRS661 for two days and

infected with HIV-1_{NL-D} at day 7 after infection. **d**. Frequency of HIV-1^+ $CD4^+$ T cells incubated with different doses of IRS661 (n=5 donors in 5 independent experiments). **e**. $CD4^+$ T cells were stimulated with anti-CD3 and anti-CD28 in the presence of two TLR7 shRNA (clones 3 and 4) or non-target control (NT) and after two days the cells were infected with HIV-1 or mock (left panel). Dot plots show a representative example of IFN-γ and IL-2 secretion after a four-hour PMA and ionomycin stimulation at day 7 after infection. **f.** Frequency of IL-2- and IFN-γ-producing $CD4^+$ T cells (n=4 donors in 4 independent experiments). **g.** Anergy-related gene expression on HIV-1^+CD4^+ T cells *in vitro* infected with HIV-1 in the presence of IRS661 or a control sequence. HIV-1^+ cells were sorted at day 7 after infection (n=6 donors in 6 independent experiments). **h.** $CD4^+$ T cells were pre-incubated with Quin-2 AM and infected with HIV-1. Dot plots show the frequency of viable HIV-1^+CD4^+ T cells at day 7 after infection. Right diagram shows the kinetic analysis of 6 independent experiments performed with one donor each. **i.** $CD4^+$ T cells were stimulated in the presence of two NFAT1-specific shRNA (middle and right dot plots) or a non-target shRNA as a control (left dot plot) and infected with HIV-1 two days later. Dot plots show the frequency of viable HIV-1^+CD4^+ T cells at day 7 after infection. Diagram on the right shows the statistical analysis of 6 independent experiments performed with one donor each. **j.** $CD4^+$ T cells were pre-incubated with VIVIT peptide and infected with HIV-1. Dot plots show the frequency of viable HIV-1^+CD4^+ T cells at day 7 after infection. Right diagram shows the kinetic analysis of 6 independent experiments performed with one donor each, shown as mean±s.e.m. * $p<0.05$, ** $p<0.005$, *** $p<0.0005$.

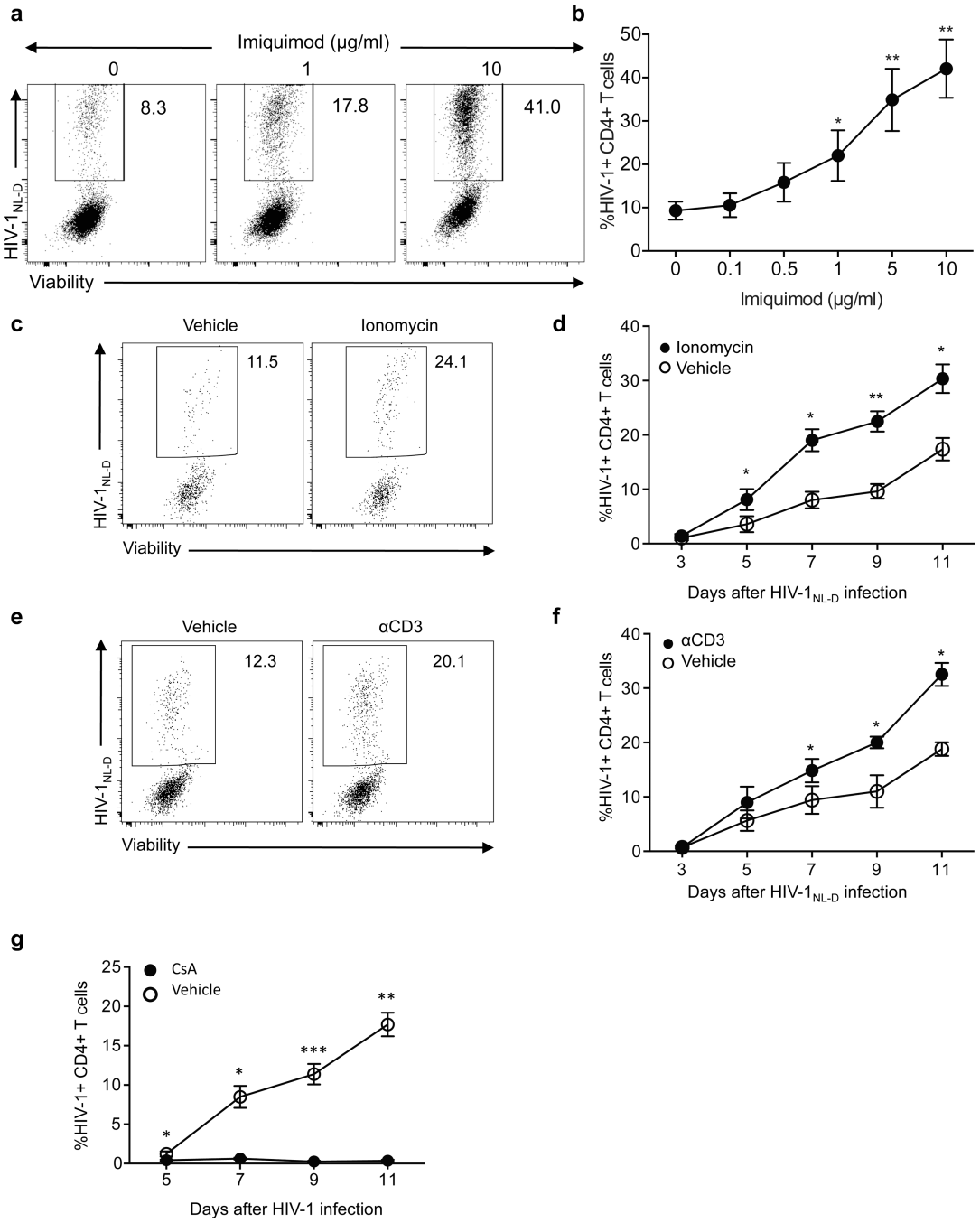

Figure 7.

Calcium-induced anergy favors HIV-1 replication. **a**. $CD4^+$ T cells were stimulated in the presence of different doses of IMQ for two days and infected with HIV-$1_{NL\text{-}D}$. Dot plots show a representative example of frequency of viable HIV-1^+ $CD4^+$ T cells at day 7 after infection. **b**. Dose-dependent effect of IMQ on the frequency of HIV-1^+ $CD4^+$ T cells (n=3 independent experiments with one donor each). **c.** Frequency of viable HIV-1^+CD4^+ T cells pre-incubated with ionomycin (right) or vehicle (left) and infected with HIV-1 at day 9 after infection. **d.** Kinetic analysis of the frequency of HIV-1^+ $CD4^+$ T cells pre-incubated with

ionomycin (n=6 donors in 6 independent experiments). **e.** Frequency of viable HIV-$1^{+}CD4^{+}$ T cells pre-incubated with anti-CD3 (right) or vehicle (left) and infected with HIV-1 at day 9 after infection. **f.** Kinetic analysis of the frequency of HIV-1^{+} $CD4^{+}$ T cells pre-incubated with anti-CD3 (n=6 donors in 6 independent experiments). **g.** $CD4^{+}$ T cells were stimulated with anti-CD3 and anti-CD28 for two days and cyclosporine was added to the cultures six hours before HIV-1 infection. Diagrams show the frequency of HIV-1-infected $CD4^{+}$ T cells after cyclosporine addition at different time points as mean±s.e.m. (n=6 donors in 6 independent experiments)* $p<0.05$, ** $p<0.005$, *** $p<0.0005$.

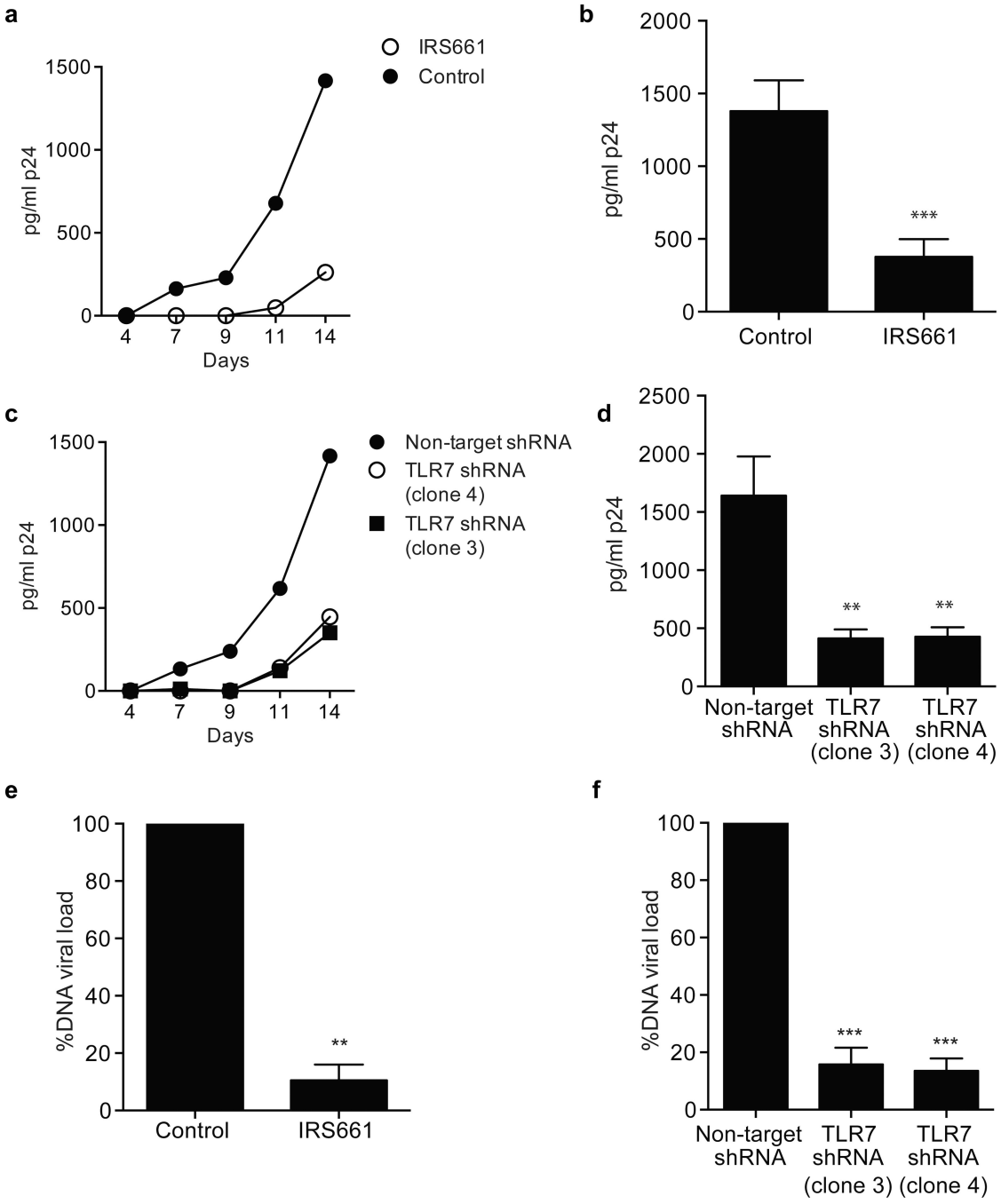

Figure 8. TLR7 inhibition decreases infection in HIV-1$^+$ patients

a. p24 concentration at different time points in CD4$^+$ T cells isolated from a representative HIV-1-infected patient and stimulated for 14 days in the presence of IRS661 (open circle) or control sequence (black). **b**. p24 concentration at day 14 in CD4$^+$ T cells isolated from HIV-1-infected patients and stimulated in the presence of IRS661 or a control (Ctrl) sequence (9 patients in 7 independent experiments). **c**. p24 concentration at different time points in CD4$^+$ T cells isolated from a representative HIV-1-infected patient and stimulated for 14 days in the presence of a non-specific target shRNA (NT) or two different TLR7

shRNA clones (TLR7 (3) and (4)). **d**. p24 concentration at day 14 in $CD4^+$ T cells isolated from HIV-1-infected patients and stimulated in the presence of of a non-specific target shRNA (NT) or two different TLR7 shRNA clones (n=9 patients in 7 independent experiments). **e**. DNA proviral load in $CD4^+$ T cells from five HIV-1-infected patients stimulated for 11 days in the presence of IRS661 or a control (Ctrl) sequence. **f**. DNA proviral load in $CD4^+$ T cells from five HIV-1-infected patients stimulated for 11 days in the presence of a non-target shRNA (NT) or two TLR7-specific shRNAs. * $p<0.05$, ** $p<0.005$, *** $p<0.0005$. Errors bars represent mean ± s.e.m.